An accurate density functional theory for the vapor-liquid interface of associating chain molecules based on the statistical associating fluid theory for potentials of variable range

Guy J. Gloor and George Jackson[a)]
Department of Chemical Engineering and Chemical Technology, Imperial College London, South Kensington Campus, London SW7 2AZ, United Kingdom

Felipe J. Blas
Departamento de Física Aplicada, Facultad de Ciencias Experimentales, Universidad de Huelva, 21071 Huelva, Spain

Elvira Martín del Río
Departamento de Ingeniería Eléctrica y Térmica, Escuela Politécnica Superior de La Rábida, Universidad de Huelva, 21819 Huelva, Spain

Enrique de Miguel
Departamento de Física Aplicada, Facultad de Ciencias Experimentales, Universidad de Huelva, 21071 Huelva, Spain

(Received 21 June 2004; accepted 25 August 2004)

A Helmholtz free energy density functional is developed to describe the vapor-liquid interface of associating chain molecules. The functional is based on the statistical associating fluid theory with attractive potentials of variable range (SAFT-VR) for the homogenous fluid [A. Gil-Villegas, A. Galindo, P. J. Whitehead, S. J. Mills, G. Jackson, and A. N. Burgess, J. Chem. Phys. **106**, 4168 (1997)]. A standard perturbative density functional theory (DFT) is constructed by partitioning the free energy density into a reference term (which incorporates all of the short-range interactions, and is treated locally) and an attractive perturbation (which incorporates the long-range dispersion interactions). In our previous work [F. J. Blas, E. Martín del Río, E. de Miguel, and G. Jackson, Mol. Phys. **99**, 1851 (2001); G. J. Gloor, F. J. Blas, E. Martín del Río, E. de Miguel, and G. Jackson, Fluid Phase Equil. **194**, 521 (2002)] we used a mean-field version of the theory (SAFT-HS) in which the pair correlations were neglected in the attractive term. This provides only a qualitative description of the vapor-liquid interface, due to the inadequate mean-field treatment of the vapor-liquid equilibria. Two different approaches are used to include the correlations in the attractive term: in the first, the free energy of the homogeneous fluid is partitioned such that the effect of correlations are incorporated in the local reference term; in the second, a density averaged correlation function is incorporated into the perturbative term in a similar way to that proposed by Toxvaerd [S. Toxvaerd, J. Chem. Phys. **64**, 2863 (1976)]. The latter is found to provide the most accurate description of the vapor-liquid surface tension on comparison with new simulation data for a square-well fluid of variable range. The SAFT-VR DFT is used to examine the effect of molecular chain length and association on the surface tension. Different association schemes (dimerization, straight and branched chain formation, and network structures) are examined separately. The surface tension of the associating fluid is found to be bounded between the nonassociating and fully associated limits (both of which correspond to equivalent nonassociating systems). The temperature dependence of the surface tension is found to depend strongly on the balance between the strength and range of the association, and on the particular association scheme. In the case of a system with a strong but very localized association interaction, the surface tension exhibits the characteristic ''*s* shaped'' behavior with temperature observed in fluids such as water and alkanols. The various types of curves observed in real substances can be reproduced by the theory. It is very gratifying that a DFT based on SAFT-VR free energy can provide an accurate quantitative description of the surface tension of both the model and experimental systems. © *2004 American Institute of Physics.* [DOI: 10.1063/1.1807833]

I. INTRODUCTION

There has been a great deal of effort in developing equations of state that can be used to describe the thermodynamics and bulk phase equilibria of fluids and fluid mixtures. The early perturbative and integral equation approaches accurately describe relatively simple systems of spherical molecules with isotropic attractive interactions such as the Lennard-Jones fluid.[1] Analytical theories have now been developed to provide a quantitative description of bulk fluids

[a)]Author to whom correspondence should be addressed; Electronic mail: g.jackson@imperial.ac.uk

comprising molecules with more complex interactions such as associating systems, amphiphiles, polymers, and electrolytes (the reader is directed to the excellent reviews in the collection by Sengers *et al.*[2]). A very successful modern equation of state for complex fluids is the statistical associating fluid theory (SAFT) (Refs. 3 and 4) which is based on Wertheim's first-order perturbation theory (TPT1) for associating systems.[5–8] The SAFT approach and its many extensions have been shown to be very versatile, describing the fluid phase behavior of systems ranging from small strongly associating molecules such as water, to long-chain alkanes, polymers, and electrolytes (see the comprehensive reviews by Müller and Gubbins[9,10]).

Though the study of inhomogeneous fluids has a long history from the early mechanical treatment of Laplace and Young,[11] through the square gradient approach of van der Waals,[11,12] to the present day molecular density functional theories (DFTs),[13] a quantitative description of the interfacial properties of inhomogeneous fluids such as the interfacial thickness, adsorption, wetting, and the surface tension is relatively rare, particularly in the case of molecules with complex interactions. Interfacial systems are ubiquitous in living systems (cell membranes are interfaces which control molecular transport and biological function) and are of fundamental industrial importance in areas as diverse as detergency (surfactants and solubilization), food production (emulsions and colloids), cosmetics (structures phases), and optoelectronic devices (liquid crystals). The development of quantitative theories of inhomogeneous systems comprising nonspherical molecules with anisotropic interactions is therefore particularly timely.

The molecular statistical mechanics of interfaces is now very well developed. In the case of inhomogeneous systems the free energy becomes a functional of the spatially varying density. The most popular and successful molecular description of interfacial systems invariably involves a DFT treatment. The DFT approach has been described in detail by a number of authors including Evans,[13] Davis,[14] and Winkelmann,[15] who have discussed the general formalism and the various approximations including perturbation expansions, the local density approximation (LDA), and the weighted density approximation (WDA). The latter is necessary when dealing with highly oscillatory density profiles, as found in fluids close to a solid surface or in a confined geometry. In our case we are interested in the vapor-liquid interface, and the LDA treatment is expected to provide a good description of the interfacial profile and surface tension for temperatures away from the triple point. Standard DFTs are based on a perturbation about a reference system, and the long-range dispersion interactions are included as a perturbative term. If correlations are neglected in this attractive term, the DFT reduces to a mean-field (van der Waals) treatment.[16] Compared to the effort devoted to the development of an accurate description of the reference term (e.g., with the use of WDAs),[13,15] less attention has been placed on the incorporation of correlations in the perturbative term since the early work of Toxvaerd.[17–19] An adequate treatment of the correlations in the attractive term is crucial for an accurate description of both the fluid phase equilibria and the interfacial properties. Toxvaerd performed a full integration over the hard-sphere reference system using an average pair distribution function of the inhomogeneous system. Similar averaging procedures for the inhomogeneous correlation function of the reference system have now been employed by Carey *et al.*,[20] Tang *et al.*,[21] Sokolowski and Fischer,[22] Winkelmann and co-workers,[15,23] and by Tang and Wu.[24]

Inhomogeneous systems of associating molecules have received particular attention in recent years. Chapman[25] was the first to suggest that the Wertheim TPT1 free energy could be used naturally in a DFT treatment of inhomogeneous associating fluids. Most of the subsequent studies have focussed on confined associating systems (see Ref. 26 for a short review). The effect of association on the surface tension of the vapor-liquid interface is a rich and relatively unexplored area of study. The link between the highly directional attractive interactions at the molecular level and the interfacial properties is still poorly understood. In their classic monograph, Rowlinson and Widom[11] give a brief discussion of the ''*s* shape'' behavior of the surface tension as a function of temperature exhibited by strongly associating fluids such as water: here the anomalous behavior is seen as a ''pale reflection'' of the unusual density and compressibility effects found in water. An alternative explanation is given by Yang *et al.*[27] in terms of the surface entropy. Their argument for the orientational ordering of water molecules at the interface is a strong one, but the relationship between this ordering and the surface tension is less clear. The mean-field theory used by Yang *et al.* includes the polar interactions explicitly, but cannot reproduce the ''*s* shape'' behavior in the surface tension of water. An extended van der Waals treatment has also been used to describe the interfacial properties of water where the effect of hydrogen bonding is included in an approximate way by counting the bonded states within a square gradient approach.[28] Though an anomalous curvature can be introduced into the temperature dependence of the surface tension of water close to the triple point, the inflection found at intermediate temperatures is not reproduced.

Mean-field versions of Wertheim's theory of association have also been incorporated into density functional theories in studies of the vapor-liquid interface of associating compounds.[26,29–34] Borowko *et al.*[29] have examined the effect of dimerization on the density profile of a fluid with a single bonding site; as was also found by Blas *et al.*,[26] the profile of the fraction of molecules not bonded is found to be shifted slightly towards the vapor phase. Pizio *et al.*[31] undertook a study with a similar theory to examine the effect of confinement on the vapor-liquid interface for two-site associating Lennard-Jones molecules which bond to form chain-like structures. In our previous papers[26,34] an inhomogenous van der Waals DFT based on the mean-field SAFT free energy (SAFT-HS) (Refs. 35–37) was used to examine the effect of association on the density profiles and surface tension. We concluded that molecular association sharpens the interface and leads to an increase in the surface tension. The curve of the surface tension with temperature was also found to be bounded between the nonassociating and associating limits; the range of the dispersive interactions is the key pa-

rameter in determining the slope of the curve.[34] Talanquer and Oxtoby[30] have used essentially the same free energy functional to study the nucleation of liquids of single-site dimerizing spherical molecules by examining the surface tension of the system. In another relevant paper, Peery and Evans[32] have studied a system of hard-core Lennard-Jones spheres with a single associating site using Wertheim's theory within a local square gradient approximation. They concluded that although molecular association has little effect on the density profile, it has a significant effect on the surface tension. Peery and Evans also suggest that the surface tension can decrease with increasing association, a counterintuitive conclusion that is a result of examining the behavior of the surface tension in terms of a scaled temperature (cf. Ref. 26). We will return to this subtle but important point later. The square gradient treatment[11,12,20,38–40] has also been employed with the SAFT free energy to examine the interfacial properties of a number of real molecules.[41–44] Though the square-gradient SAFT approach has been shown to provide a good representation of the surface tension of a number of pure fluids and mixtures, this requires the use of empirical adjustable parameters (the so-called ''influence'' parameters) which limits the predictive capabilities of the method.

The direct simulation of the vapor-liquid surface tension of associating fluids is comparatively rare. Alejandre *et al.*[33] have examined a one-site dimerizing Lennard-Jones system, and determined the surface tension from the mechanical route by calculating the pressure tensor. The effect of association on the density profile and surface tension is consistent with the findings of Blas *et al.*[26] An examination of the density profile of the unbonded molecules (monomers) revealed the presence of a small peak which suggests that the monomers tend to accumulate at the interface; this appears to be related to the shift of the profile for the fraction of monomers to the vapor side of the interface,[26] but the effect was not noted in subsequent work. Tapia-Medina *et al.*[45] also compared the density profiles and surface tension for dimerizing Yukawa fluids with the results determined with the SAFT-HS mean-field DFT;[26] though qualitative agreement is found the theory does not provide an accurate description of the surface tension (as expected for a mean-field theory). In a complementary and interesting simulation study, Singh and Kofke[46] have used the transition-matrix grand-canonical Monte Carlo technique to provide a particularly thorough examination of the effect of association on the surface tension of dimerizing square-well molecules for different ranges and strengths of the association interaction. The behavior of the fraction of monomers along the coexistence curve and the surface tension does not appear to follow some of the predictions of Blas *et al.*[26] One should note, however, that the intermolecular parameters of the two studies are different; the fraction of monomers is very sensitive to both the strength of the interaction and the bonding volume (see Ref. 35). At this stage it is important to reemphasize that DFTs formulated at the mean-field level [such as the SAFT-HS DFT (Ref. 26)] only provide a qualitative description of the bulk fluid phase equilibria (e.g., see Refs. 15, 24, and 47). As a consequence the limiting behavior of the density profile away from the interface (which corresponds to the bulk coexisting vapor and liquid states) is not correctly represented, and surface tension can only be described at the qualitative level within the mean-field approach.

One of the main goals of the present work is to improve on the mean-field description of both the bulk phase behavior and the interfacial properties by incorporating correlations in the attractive term. In this paper we follow a standard perturbative DFT approach[13] to develop a free energy functional for inhomogeneous associating chainlike fluids based on the SAFT-VR free energy for chains formed from spherical segments with attractive interactions of variable range.[47,48] We opt for the SAFT-VR description of the reference bulk fluid as it has already been shown to provide an excellent quantitative description of the vapor-liquid and liquid-liquid fluid phase equilibria of a wide variety of systems including alkanes and perfluoroalkanes,[47,49–52] replacement refrigerants,[53] water,[54] hydrogen chloride,[55] hydrogen fluoride,[56,57] carbon dioxide,[58,59] xenon,[60–64] boron trifluoride,[65] aqueous electrolytes,[54,66] and polyethylene polymers.[67–69] An adequate treatment of the correlations in the attractive term is crucial for an accurate description of both the bulk fluid phase equilibria and the interfacial properties (cf. Ref. 15). The correlations are included in the DFT using an average bulk pair distribution function similar to that employed by Toxvaerd.[19] An accurate theory for the vapor-liquid interfacial profiles and surface tension of associating molecules with dispersion interactions of variable range can be obtained in this way. The adequacy of the theory is assessed by comparing the interfacial properties obtained from the SAFT-VR DFT with recent simulation results for square-well spherical molecules of variable range.[70,71] We also provide a detailed examination of the effect of association on the surface tension for different types of association schemes (dimerization, chain formation, and network structures). The development of a DFT based on the SAFT-VR description of bulk associating fluids is essential in providing a predictive platform for the calculation of the surface tension of real compounds. This is seen as the first step in developing a general theory of vapor-liquid and liquid-liquid interfaces of multicomponent systems and micellization.

The rest of the paper is organized as follows: in Sec. II we present the most relevant features of the molecular model and theory; the results and discussion are presented in Sec. III; and the conclusions are made in Sec. IV.

II. THEORY

In this work we consider chains of m tangent spherical segments of diameter σ which can interact through pair-wise repulsive, attractive, and associative contributions. The repulsive and attractive interactions acting on each spherical segment are described by a simple square-well potential:

$$\phi(r)=\begin{cases}\infty & r\leqslant\sigma\\ -\varepsilon & \sigma<r\leqslant\lambda\sigma,\\ 0 & r>\lambda\sigma\end{cases} \tag{1}$$

where r denotes the distance between the centers of the two segments, and $\lambda\sigma$ denotes the range of the attractive interaction of depth $-\varepsilon$. In the SAFT-VR approach the variable range of the attractive interactions plays an important role in describing the interactions of molecules with varying degrees of polarity.[47] The association (hydrogen bonding) contribution is modeled by considering additional off-center sites (placed a distance r_d from the center of a given segment) which interact through a square-well potential of shorter range r_c; the interaction of a site A on one segment with a site B on another is given by

$$\phi_{AB}(r)=\begin{cases}-\varepsilon_{AB} & r_{AB}<r_c\\ 0 & r_{AB}>r_c\end{cases}. \tag{2}$$

In spite of its simplicity, this model includes the relevant features found in associating chain molecules: repulsive, attractive, and associative interactions.

A. Homogeneous fluid of associating chain molecules (SAFT-VR)

Within the SAFT-VR approach the Helmholtz free energy A of the homogeneous fluid is written as a perturbation expansion which takes into account the varios types of interactions. In the case of associating molecules, A can be expressed as a sum of an ideal contribution A^{ideal}, a monomer term A^{mono} (which takes into account the attractive and repulsive forces between the segments that form the molecules), a chain contribution A^{chain} (which accounts for the connectivity of the segments in the molecules), and a contribution due to association A^{assoc}:[47]

$$a=\frac{A}{Nk_BT}=\frac{A^{\text{ideal}}}{Nk_BT}+\frac{A^{\text{mono}}}{Nk_BT}+\frac{A^{\text{chain}}}{Nk_BT}+\frac{A^{\text{assoc}}}{Nk_BT}, \tag{3}$$

where N is the number of chain molecules (each comprising m spherical segments), T is the temperature, and k_B is the Boltzmann constant.

1. Ideal contribution

The ideal term is given in the standard form as[72]

$$a^{\text{ideal}}(\rho)\equiv\frac{A^{\text{ideal}}}{Nk_BT}=\ln(\rho\Lambda^3)-1, \tag{4}$$

where $\rho=N/V$ is the number density of chain molecules, and Λ is a thermal de Broglie wavelength which contains the translational and rotational contributions to the partition function of the ideal chain; the kinetic contributions do not have to be specified explicitly as they do not contribute to the fluid-phase equilibria and interfacial properties.

2. Monomer contribution

The term A^{mono} combines the repulsive and attractive contributions to the free energy of the monomeric spherical segments making up the chain molecules. A high-temperature Barker and Henderson[73,74] perturbation expansion (truncated at second order) about a hard-sphere reference system is used to describe the free energy of the monomers:

$$a^{\text{mono}}(\rho)\equiv\frac{A^{\text{mono}}}{Nk_BT}=m(a^{\text{hs}}+a_1+a_2). \tag{5}$$

The factor m appears in the expression because the monomer free energy is given in terms of the number of chain molecules N and not of the number of spherical segments $N_s=mN$.

The reference hard-sphere term is obtained from the Carnahan-Starling expression,[75,76]

$$a^{\text{hs}}(\rho)\equiv\frac{A^{\text{hs}}}{N_sk_BT}=\frac{4\eta-3\eta^2}{(1-\eta)^2}, \tag{6}$$

where $\eta=\pi\sigma^3\rho_s/6=\pi\sigma^3m\rho/6$ is the usual packing fraction and $\rho_s=N_s/V$ is the number density of segments.

The mean-attractive energy a_1 is defined as

$$a_1(\rho)\equiv\frac{A_1}{N_sk_BT}=-\frac{2\pi\rho_s}{k_BT}\int_\sigma^\infty dr\,r^2\phi(r)g^{\text{hs}}(r;\rho), \tag{7}$$

where $g^{\text{hs}}(r;\rho)$ is the pair radial distribution function of the reference hard-sphere fluid. One can factorize the pair distribution function out of the integral by employing the mean-value theorem, and write the expression in terms of a contact value of the system at an effective density ρ_{eff} (or effective packing fraction, $\eta_{\text{eff}}=\pi\sigma^3m\rho_{\text{eff}}/6$):[47]

$$a_1=a_1^{\text{vdW}}g^{\text{hs}}(\sigma;\rho_{\text{eff}}). \tag{8}$$

The prefactor a_1^{vdW} is the van der Waals attractive free energy (representing the long-range contribution for a system without correlations) and is given by

$$a_1^{\text{vdW}}=-\frac{2\pi\rho_s}{k_BT}\int_\sigma^\infty dr\,r^2\phi(r), \tag{9}$$

which for the square-well potential becomes

$$a_1^{\text{vdW}}=\frac{2}{3}\frac{\pi\rho_s}{k_BT}\sigma^3\varepsilon(\lambda^3-1). \tag{10}$$

The contact value of the pair distribution for the hard-sphere fluid at the effective density ρ_{eff} (or correspondingly at the effective packing fraction η_{eff}) is given by[47]

$$g^{\text{hs}}(\sigma;\rho_{\text{eff}})=\frac{1-\eta_{\text{eff}}/2}{(1-\eta_{\text{eff}})^3}. \tag{11}$$

The dependence of η_{eff} on the actual packing fraction η and the range of the square-well potential λ is obtained by using a very accurate description of the structure of the hard-sphere reference system with the following parametrization,

$$\eta_{\text{eff}}=c_1\eta+c_2\eta^2+c_3\eta^3, \tag{12}$$

where the coefficients c_n are obtained from the matrix

$$\begin{pmatrix}c_1\\ c_2\\ c_3\end{pmatrix}=\begin{pmatrix}2.258\,55 & -1.053\,49 & 0.249\,434\\ -0.692\,70 & 1.400\,49 & -0.827\,739\\ 10.1576 & -15.0427 & 5.30827\end{pmatrix}\begin{pmatrix}1\\ \lambda\\ \lambda^2\end{pmatrix}. \tag{13}$$

As it will become clear in Sec. II B 2, it is useful to partition the mean-attractive energy $a_1(\rho)=a_1^{\text{sr}}(\rho)+a_1^{\text{lr}}(\rho)$

into short-range (a_1^{sr}) and long-range (a_1^{lr}) parts. The short-range contribution is written in terms of the total correlation function $h^{hs}(r;\rho)=g^{hs}(r;\rho)-1$ as

$$a_1^{sr}(\rho)=-\frac{2\pi\rho_s}{k_BT}\int_\sigma^\infty drr^2\phi(r)h^{hs}(r;\rho), \tag{14}$$

and is seen to incorporate the local structure of the fluid. The long-range contribution is simply represented by the van der Waals attractive term $a_1^{lr}\equiv a_1^{vdW}$ [cf. Eq. (9)].

The second-order perturbation (fluctuation) term is expressed in terms of the local compressibility approximation (LCA) of Barker and Henderson[77] where the fluctuation of the energy is related directly to the compressibility of the system by

$$a_2(\rho)\equiv\frac{A_2}{N_sk_BT}=\frac{1}{2}\frac{\varepsilon}{k_BT}K^{hs}\eta a_1'. \tag{15}$$

In this relation $a_1'(\rho)=\partial a_1/\partial\eta$ represents the density derivative of the mean-attractive energy, and K^{hs} is the Percus-Yevick expression for the hard-sphere compressibility factor given by[76]

$$K^{hs}=\frac{(1-\eta)^4}{1+4\eta+4\eta^2}. \tag{16}$$

The SAFT-HS monomer contribution to the Helmholtz free energy is simply obtained from the SAFT-VR free energy by ignoring the correlations between the spherical segments [which amounts to setting $g^{hs}(r;\rho)=1$ in the expression for the mean-attractive energy given by Eq. (7)], as well as ignoring the fluctuations of the attractive energy ($a_2=0$). This corresponds to the well known van der Waals mean-field approximation.

3. Chain contribution

The contribution to the free energy due to the formation of a chain molecule of m square-well segments is given in the standard Wertheim TPT1 form as[78]

$$a^{chain}(\rho)\equiv\frac{A^{chain}}{Nk_BT}=-(m-1)\ln y^{sw}(\sigma;\rho), \tag{17}$$

where $y^{sw}(\sigma;\rho)=\exp(-\varepsilon/k_BT)g^{sw}(\sigma;\rho)$ is the contact value of the background (cavity) pair correlation function for a system of square-well monomers. In the SAFT-VR approach the contact value of the pair radial distribution function $g^{sw}(\sigma;\rho)$ is obtained from a first-order high-temperature expansion about a hard-sphere reference system:[47]

$$g^{sw}(\sigma;\rho)=g^{hs}(\sigma;\rho)+\frac{1}{4}\left[\frac{\partial a_1}{\partial\eta}-\frac{\lambda}{3\eta}\frac{\partial a_1}{\partial\lambda}\right]. \tag{18}$$

The contact value $g^{hs}(\sigma;\rho)$ of the correlation function for the hard-sphere system is represented by the Carnahan and Starling expression:[75,76]

$$g^{hs}(\sigma;\rho)=\frac{1-\eta/2}{(1-\eta)^3}. \tag{19}$$

In the case of the SAFT-HS approach the monomer contact pair radial distribution function that is used in the chain contribution to the free energy [Eq. (17)] is approximated simply by that of the hard-sphere system [$g^{sw}(r;\rho)\approx g^{hs}(r;\rho)$, i.e., the first term of Eq. (18)]. The contribution to the free energy that is described here is obtained from the Wertheim treatment of an associating system in limit of complete bonding.[36,79]

4. Association contribution

The association contribution to the free energy, which constitutes the core of all SAFT equations of state, is described with the Wertheim theory of association.[5–8] This term can be expressed as a function of the fraction of molecules not bonded at given sites as[35]

$$a^{assoc}(\rho)\equiv\frac{A^{assoc}}{Nk_BT}=\left[\sum_{A=1}^{n}\left(\ln X_A-\frac{X_A}{2}\right)+\frac{1}{2}n\right], \tag{20}$$

where X_A is the fraction of molecules not bonded at a given site A and n is the total number of sites on each molecule. The fraction of molecules not bonded at each site is calculated by solving the following set of coupled mass-action equations,

$$X_A=\frac{1}{1+\Sigma_{B=1}^{n}X_B\rho\Delta_{AB}}, \tag{21}$$

where B denotes the set of sites capable of bonding with site A. The association interaction parameter Δ_{AB} is determined from the Mayer function $F_{AB}=[\exp(\varepsilon_{AB}/k_BT)-1]$, the volume K_{AB} available for bonding between sites A and B, and the contact value of the monomer pair radial distribution function:

$$\Delta_{AB}=F_{AB}K_{AB}g^{sw}(\sigma;\rho). \tag{22}$$

The explicit dependence of the bonding volume on the distance $r_d^*=r_d/\sigma$ of the site from the center of the spherical segment and the range $r_c^*=r_c/\sigma$ of the site-site interaction can be expressed analytically as[35]

$$\begin{aligned}K_{AB}=\frac{4\pi\sigma^3}{72r_d^{*2}}&[\ln(r_c^*+2r_d^*)(6r_c^{*3}+18r_c^{*2}r_d^*-24r_d^{*3})\\&+(r_c^*+2r_d^*-1)(22r_d^{*2}-5r_c^*r_d^*-7r_d^*-8r_c^{*2}\\&+r_c^*+1)].\end{aligned} \tag{23}$$

In the case of the SAFT-HS description the contact value of the monomer pair radial distribution function appearing in Eq. (22) is again approximated by the hard-sphere value, $g^{sw}(\sigma;\rho)\approx g^{hs}(\sigma;\rho)$.

The free energy that has been described for the homogeneous fluid of associating chain molecules can be used to determine the bulk vapor-liquid equilibria in a straightforward fashion. The densities of the coexisting vapor and liquid states at a fixed temperature are determined numerically by requiring that the pressure $P=-(\partial A/\partial V)_{T,N}$, and chemical potential $\mu=-(\partial A/\partial N)_{T,V}$ of the two phases are equal.

Now that the contributions to the free energy of the bulk fluid of associating chain molecules have been defined we are in a position to construct the perturbative free energy functional for the inhomogeneous fluid.

B. Inhomogeneous fluid of associating chain molecules (SAFT DFT)

We consider an open system at temperature T and chemical potential μ in a volume V. In the absence of external fields, the grand potential functional $\Omega[\rho(\mathbf{r})]$ of an inhomogeneous system is given by[13]

$$\Omega[\rho(\mathbf{r})]=A[\rho(\mathbf{r})]-\mu\int d\mathbf{r}\rho(\mathbf{r}), \tag{24}$$

where $A[\rho(\mathbf{r})]$ is the intrinsic Helmholtz free energy functional. The minimum value of $\Omega[\rho(\mathbf{r})]$ is the equilibrium grand potential of the system and the corresponding equilibrium density profile $\rho_{eq}(\mathbf{r})$ satisfies the following condition:[13]

$$\left.\frac{\delta\Omega[\rho(\mathbf{r})]}{\delta\rho(\mathbf{r})}\right|_{eq}=\left.\frac{\delta A[\rho(\mathbf{r})]}{\delta\rho(\mathbf{r})}\right|_{eq}-\mu=0. \tag{25}$$

In essence this Euler-Lagrange equation is equivalent to requiring that the Helmholtz free energy functional be a minimum subject to a constraint of constant number of particles; the undetermined multiplier corresponds to the chemical potential μ of the bulk coexisting phases.

Following a standard perturbative approach[13,15] the free energy is partitioned into a reference term (which includes the ideal, hard-sphere, chain, and associative contributions), and a perturbation attractive term (which includes the dispersive interactions between the monomeric segments). In this work we consider three different levels of approximation to account for the description of the vapor-liquid interface. In the first approach (SAFT-VR DFT), both the bulk vapor-liquid equilibria and the interfacial properties are described with a perturbation theory in which correlations are included in the reference and attractive terms. In the second approximation scheme (SAFT-VR MF DFT), the bulk fluid is treated at the SAFT-VR level (a second-order perturbation theory which incorporates the correlations of the hard-sphere reference system), while the interfacial properties are treated at the mean-field level (the correlations are neglected in the attractive term). Finally, in the third approach (SAFT-HS MF DFT) both the bulk and interfacial properties are described at the mean-field level as far as the attractive dispersive forces are concerned. The latter approximation corresponds to the SAFT-HS free energy functional described in Refs. 26 and 34.

1. SAFT-VR DFT

The reduced Helmholtz free energy functional in the full SAFT-VR treatment of associating chain molecules describes both the bulk vapor-liquid equilibria and the interfacial properties within a perturbation approach. Correlations are taken into account explicitly both in the reference and attractive terms. The full SAFT-VR free energy functional is given by

$$A^{\text{SAFT-VR}}[\rho(\mathbf{r})]=A^{\text{ideal}}[\rho(\mathbf{r})]+A^{\text{ref}}_{\text{VR}}[\rho(\mathbf{r})]+A^{\text{att}}_{\text{VR}}[\rho(\mathbf{r})]. \tag{26}$$

It is convenient to examine the grand potential functional in terms of reduced free energy densities $f[\rho(\mathbf{r})]\equiv A[\rho(\mathbf{r})]/Vk_BT\equiv\rho(\mathbf{r})a[\rho(\mathbf{r})]$, where $a[\rho(\mathbf{r})]\equiv A[\rho(\mathbf{r})]/(Nk_BT)$.

The reduced ideal Helmholtz free energy of an inhomogeneous system of nonspherical particles can be written as[13,76]

$$A^{\text{ideal}}[\rho(\mathbf{r})]=k_BT\int d\mathbf{r}f^{\text{ideal}}(\rho(\mathbf{r}))$$

$$=k_BT\int d\mathbf{r}\rho(\mathbf{r})a^{\text{ideal}}(\rho(\mathbf{r})), \tag{27}$$

where the form of the density dependence of $a^{\text{ideal}}(\rho(\mathbf{r}))$ is given by Eq. (4).

As in our previous work[26,34] the reference term $A^{\text{ref}}_{\text{VR}}$ is taken to incorporate all of the contributions to the free energy due to ''short-range'' interactions such as the repulsive hard-sphere term, the chain term, and the association term:

$$A^{\text{ref}}_{\text{VR}}[\rho(\mathbf{r})]=A^{\text{hs}}[\rho(\mathbf{r})]+A^{\text{chain}}[\rho(\mathbf{r})]+A^{\text{assoc}}[\rho(\mathbf{r})]$$

$$+A_2[\rho(\mathbf{r})]. \tag{28}$$

The hard-sphere interaction is short ranged and is usually treated locally in a perturbative DFT treatment of the vapor-liquid interface;[13,15] such functionals based on the LDA of the reference term provide a good description of the vapor-liquid interface, although the approach fails for fluids close to their triple points or for confined systems where a WDA has to be used. In our SAFT-VR DFT the hard-sphere LDA free energy functional is given by

$$A^{\text{hs}}[\rho(\mathbf{r})]=k_BT\int d\mathbf{r}f^{\text{hs}}(\rho(\mathbf{r}))$$

$$=k_BT\int d\mathbf{r}\rho(\mathbf{r})ma^{\text{hs}}(\rho(\mathbf{r})), \tag{29}$$

where the expression for $a^{\text{hs}}(\rho(\mathbf{r}))$ is written as a function of the packing fraction profile $\eta(\mathbf{r})=(m\pi\sigma^3/6)\rho(\mathbf{r})$ in the Carnahan and Starling form [cf. Eq. (6)]. The factor of m was erroneously omitted from Eq. (8) in Ref. 26.

Both the hard-chain [cf. Eq. (17)] and the association [cf. Eq. (20)] contributions to the SAFT free energy can be written in terms of the contact value of the pair radial distribution function of the reference monomer system; this is clearly a short-range contribution and can also be approximated by a local functional. The contribution to the reference free energy functional for the formation of a chain of m square-well segments is written at the LDA level as

$$A^{\text{chain}}[\rho(\mathbf{r})]=k_BT\int d\mathbf{r}\,f^{\text{chain}}(\rho(\mathbf{r}))$$

$$=k_BT\int d\mathbf{r}\,\rho(\mathbf{r})a^{\text{chain}}(\rho(\mathbf{r})), \tag{30}$$

where $a^{\text{chain}}(\rho(\mathbf{r}))$ is the function of density given by Eq. (17). The LDA treatment of long chains may appear to be rather drastic. As will be shown later, it nonetheless provides a good description of the vapor-liquid surface tension of moderately long alkanes. In essence this approximation

amounts to determining the average density profile for the segments making up the chain without specifying which chain the segments belong to. A more sophisticated WDA treatment, such as that developed by Kierlik and co-workers,[80–82] in which the position of each segment of the chain is treated explicitly, can be used to improve the description of long chains. This is, however, beyond the scope of the current work.

In a similar way we can write the contribution due to molecular association at the LDA level as

$$A^{\text{assoc}}[\rho(\mathbf{r})] = k_B T \int d\mathbf{r}\, f^{\text{assoc}}(\rho(\mathbf{r})) = k_B T \int d\mathbf{r}\, \rho(\mathbf{r}) a^{\text{assoc}}(\rho(\mathbf{r})), \tag{31}$$

where $a^{\text{assoc}}(\rho(\mathbf{r}))$ is given by Eq. (20). The perturbation theory of Wertheim[5–8] was originally developed in the general case of inhomogenous systems; the fraction $X_A[\rho(\mathbf{r})]$ of molecules not bonded at a given site A at a point $\mathbf{r}$ in the fluid can be expressed as a set of mass-action equations:

$$X_A[\rho(\mathbf{r})] = \frac{1}{1+\Sigma_B \int d\mathbf{r}'\, d\omega'\, \rho(\mathbf{r}') X_B[\rho(\mathbf{r}')] F_{AB} g^{\text{sw}}[\mathbf{r},\mathbf{r}';\rho(\mathbf{r}),\rho(\mathbf{r}')]}. \tag{32}$$

The mass-action equations are seen to be nonlocal in nature, i.e., the property at a point $\mathbf{r}$ depends on an integral over neighboring points $\mathbf{r}'$. The integral over orientations ω' for the site-site association interaction is also undertaken. In our local LDA treatment we assume that the density does not vary appreciably over the range of the site-site association interaction, $\rho(\mathbf{r}') \approx \rho(\mathbf{r})$; this is expected to be a good approximation for hydrogen-bonding association where the range of the interaction is very short. The LDA form of the set of mass-action equations defined by Eq. (32) can be written as

$$X_A(\rho(\mathbf{r})) = \frac{1}{1+\Sigma_B \rho(\mathbf{r}) X_B(\rho(\mathbf{r})) \Delta_{AB}}. \tag{33}$$

The correlations are included in the term Δ_{AB} where we have invoked the additional approximation that $r^2 g^{\text{sw}}[r;\rho(\mathbf{r})]$ does not vary appreciably over the range of the site-site interaction:[35]

$$\Delta_{AB} = K_{AB} F_{AB} g^{\text{sw}}[\sigma;\rho(\mathbf{r})]. \tag{34}$$

In the SAFT-VR description of the thermodynamics of the fluid, the high-temperature perturbation expansion of the free energy is taken to second order A_2. The LCA is used to approximate the fluctuation term A_2 of the homogeneous system in terms of the compressibility of the hard-sphere fluid. This contribution is also treated locally in our reference term,

$$A_2[\rho(\mathbf{r})] = k_B T \int d\mathbf{r}\, f_2(\rho(\mathbf{r})) = k_B T \int d\mathbf{r}\, \rho(\mathbf{r}) m a_2(\rho(\mathbf{r})), \tag{35}$$

where $a_2(\rho(\mathbf{r}))$ is given by Eq. (15). The slope of the profile for the mean attractive energy turns out to be fairly constant over the interfacial region,[70] which suggests that the fluctuation term is reasonably constant and can be treated locally since $a_1'(\rho(\mathbf{r})) \propto a_2(\rho(\mathbf{r}))$. At this stage we should point out that the second-order term has to be included in the full free energy functional of the inhomogeneous system in order to recover the SAFT-VR expressions of the homogeneous bulk phase. This term did not have to be taken into account in our previous mean-field description.[26,34]

Before we end our description of the reference free energy functional it is instructive to note that within the LDA treatment the free energy density $f^{\text{ref}}(\rho(\mathbf{r}))$ is given as a simple function, not a functional, of the local density (which is represented by that of the homogeneous system).

The usual form of the attractive term in a perturbative DFT treatment of an inhomogeneous fluid of spherical particles is[13–15]

$$A_{\text{VR}}^{\text{att}}[\rho(\mathbf{r})] = \frac{1}{2} \int d\mathbf{r}\, \rho(\mathbf{r}) \int d\mathbf{r}'\, \rho(\mathbf{r}') \times g^{\text{ref}}[\mathbf{r},\mathbf{r}';\rho(\mathbf{r}),\rho(\mathbf{r}')] \phi^{\text{att}}(|\mathbf{r}-\mathbf{r}'|). \tag{36}$$

The functional $g^{\text{ref}}[\mathbf{r},\mathbf{r}';\rho(\mathbf{r}),\rho(\mathbf{r}')]$ denotes the pair correlation function of the reference inhomogeneous system (usually a hard-sphere fluid), and the potential $\phi^{\text{att}}(|\mathbf{r}-\mathbf{r}'|)$ is the attractive part of the intermolecular potential. An extension of Eq. (36) to deal with chainlike molecules can be written as

$$A_{\text{VR}}^{\text{att}}[\rho(\mathbf{r})] = \frac{1}{2} \int d\mathbf{r}\, \rho_s(\mathbf{r}) \int d\mathbf{r}'\, \rho_s(\mathbf{r}') \times g_{\text{ss}}^{\text{hsc}}[\mathbf{r},\mathbf{r}';\rho_s(\mathbf{r}),\rho_s(\mathbf{r}')] \phi^{\text{att}}(|\mathbf{r}-\mathbf{r}'|). \tag{37}$$

The attractive contribution is now expressed in terms of the average segment density profile $\rho_s(\mathbf{r})$, the average segment-segment pair radial distribution function of the inhomogeneous reference hard-sphere chain $g_{\text{ss}}^{\text{hsc}}[\mathbf{r},\mathbf{r}';\rho_s(\mathbf{r}),\rho_s(\mathbf{r}')]$, and the segment-segment interaction defined in Eq. (1). This corresponds to the inhomogeneous version of the attractive term described by Gross and Sadowski.[83] If we further approximate the segment-segment pair radial distribution function by that of the equivalent unbonded hard-sphere system, i.e., $g_{\text{ss}}^{\text{hsc}}[\mathbf{r},\mathbf{r}';\rho_s(\mathbf{r}),\rho_s(\mathbf{r}')] \approx g^{\text{hs}}[\mathbf{r},\mathbf{r}';\rho_s(\mathbf{r}),\rho_s(\mathbf{r}')]$, and express the functional in terms of the molecular density profile (where we assume that $\rho(\mathbf{r}) = \rho_s(\mathbf{r})/m$), the attractive contribution becomes

$$A_{\mathrm{VR}}^{\mathrm{att}}[\rho(\mathbf{r})]=\frac{1}{2}\int \mathrm{d}\mathbf{r}\, m\rho(\mathbf{r})\int \mathrm{d}\mathbf{r}' m\rho(\mathbf{r}') \times g^{\mathrm{hs}}[\mathbf{r},\mathbf{r}';\rho(\mathbf{r}),\rho(\mathbf{r}')]\phi^{\mathrm{att}}(|\mathbf{r}-\mathbf{r}'|). \quad (38)$$

A further approximation is required in Eq. (38), as little is known of the pair distribution function of the inhomogeneous hard-sphere fluid. Here, we assume that the correlations can be described with the pair distribution function of a homogeneous fluid of hard spheres evaluated at an appropriate mean density $\overline{\rho}$. This way of treating the correlations in an inhomogeneous system dates back to the work of Toxvaerd.[17–19] Though a mean-field treatment (in which the correlations are ignored) is more common, the approach has now been used by a number of other groups.[15,20–24] We consider a simple arithmetic average of the density $\overline{\rho}=[\rho(\mathbf{r})+\rho(\mathbf{r}')]/2$ (also see Ref. 84). Other choices could have been used to define $\overline{\rho}$, but we found little quantitative difference. Toxvaerd[19] has emphasized that the averaging scheme employed for the correlations in the perturbative term must be invariant under particle interchange; this condition is satisfied with our simple averaging of the density. In line with the SAFT-VR treatment of the bulk fluid,[47] the pair distribution function can then be approximated by that at contact for an equivalent system with an effective density $g^{\mathrm{hs}}(|\mathbf{r}-\mathbf{r}'|;\overline{\rho}) \approx g^{\mathrm{hs}}(\sigma;\overline{\rho}_{\mathrm{eff}})$. The final expression of the attractive term used in the SAFT-VR DFT approach is given by

$$A_{\mathrm{VR}}^{\mathrm{att}}[\rho(\mathbf{r})] = \frac{1}{2}\int \mathrm{d}\mathbf{r}\, m\rho(\mathbf{r})\int \mathrm{d}\mathbf{r}' m\rho(\mathbf{r}') g^{\mathrm{hs}}(\sigma;\overline{\rho}_{\mathrm{eff}})\phi^{\mathrm{att}}(|\mathbf{r}-\mathbf{r}'|). \quad (39)$$

The relationship between the actual number density $\overline{\rho}$ and the effective density $\overline{\rho}_{\mathrm{eff}}$ (which depends on the range of the potential λ) is taken to be the same as for the homogeneous system and follows from the corresponding expressions for the packing fractions η and η_{eff}, Eqs. (12) and (13). The advantage of using this type of free energy functional is that integrations are easier to perform and as a result the method is less computationally demanding. It is also clear that the free energy given by Eq. (26) reduces to the bulk SAFT-VR expression [cf Eq. (3)] for homogeneous systems [with $\rho(\mathbf{r})=\rho_{\mathrm{bulk}}$].

As was mentioned earlier the equilibrium interfacial profile is the one that minimizes the grand potential [cf. Eq. (25)]. In the case of the SAFT-VR DFT that has just been described, the corresponding Euler-Lagrange equation is obtained as

$$\left.\frac{\delta\Omega[\rho(\mathbf{r})]}{\delta\rho(\mathbf{r})}\right|_{\mathrm{eq}}=\frac{\delta A[\rho(\mathbf{r})]}{\delta\rho(\mathbf{r})}-\mu = \frac{\delta A^{\mathrm{ideal}}[\rho(\mathbf{r})]}{\delta\rho(\mathbf{r})}+\frac{\delta A_{\mathrm{VR}}^{\mathrm{ref}}[\rho(\mathbf{r})]}{\delta\rho(\mathbf{r})} + \frac{\delta A_{\mathrm{VR}}^{\mathrm{att}}[\rho(\mathbf{r})]}{\delta\rho(\mathbf{r})}-\mu=0. \quad (40)$$

The variation of the ideal and reference contributions with respect to $\rho(\mathbf{r})$ correspond to the local chemical potentials $\mu^{\mathrm{ideal}}(\rho(\mathbf{r}))=\delta A^{\mathrm{ideal}}[\rho(\mathbf{r})]/\delta\rho(\mathbf{r})$ and $\mu^{\mathrm{ref}}(\rho(\mathbf{r}))=\delta A_{\mathrm{VR}}^{\mathrm{ref}}[\rho(\mathbf{r})]/\delta\rho(\mathbf{r})$ (which can be obtained from the corresponding expressions for the homogeneous system, through $\mu=k_BT\{a+\rho\partial a/\partial\rho\}$), while the variation of the attractive term requires a knowledge of the density derivative of the correlation function. The equilibrium profile can thus be determined by solving the equation

$$\mu=\mu^{\mathrm{ideal}}(\rho(\mathbf{r}))+\mu_{\mathrm{VR}}^{\mathrm{ref}}(\rho(\mathbf{r}))+\int \mathrm{d}\mathbf{r}' m^2\rho(\mathbf{r}') \times\left\{ g^{\mathrm{hs}}(\sigma;\overline{\rho}_{\mathrm{eff}})+\frac{1}{2}\rho(\mathbf{r})\frac{\delta g^{\mathrm{hs}}(\sigma;\overline{\rho}_{\mathrm{eff}})}{\delta\rho(\mathbf{r})}\right\}\phi^{\mathrm{att}}(|\mathbf{r}-\mathbf{r}'|), \quad (41)$$

which ensures that the chemical potential at each point in the profile is equal to the bulk chemical potential μ (see Ref. 15).

2. SAFT-VR MF DFT

It is convenient to have a general approach for the development of an accurate free energy functional where one does not have to treat the correlations in the perturbative attractive term; this would allow one to construct a DFT from any engineering equation of state of the bulk fluid which is not explicitly cast in terms of the correlations between the particles. In this section we develop such an approach within the SAFT-VR description of homogeneous fluid, though the method is not restricted to SAFT-like equations of state. One can define a free energy functional in which the bulk fluid is treated at the full SAFT-VR level (a second-order perturbation theory which incorporates the correlations of the hard-sphere reference system), and the interface is treated at the mean-field level of van der Waals (the correlations are neglected in the attractive term).

As in the preceding section the Helmholtz free energy functional is expressed in terms of an ideal, a reference, and an attractive contribution [cf. Eq. (26)]:

$$A_{\mathrm{mf}}^{\mathrm{SAFT\text{-}VR}}[\rho(\mathbf{r})]=A^{\mathrm{ideal}}[\rho(\mathbf{r})]+A_{\mathrm{VR,mf}}^{\mathrm{ref}}[\rho(\mathbf{r})] + A_{\mathrm{VR,mf}}^{\mathrm{att}}[\rho(\mathbf{r})]. \quad (42)$$

As before the ideal term $A^{\mathrm{ideal}}[\rho(\mathbf{r})]$ is given by Eq. (27). The reference term $A_{\mathrm{VR,mf}}^{\mathrm{ref}}[\rho(\mathbf{r})]$ is again treated locally, but is now defined as

$$A_{\mathrm{VR,mf}}^{\mathrm{ref}}[\rho(\mathbf{r})]=A^{\mathrm{hs}}[\rho(\mathbf{r})]+A^{\mathrm{chain}}[\rho(\mathbf{r})]+A^{\mathrm{assoc}}[\rho(\mathbf{r})] + A_1^{\mathrm{sr}}[\rho(\mathbf{r})]+A_2[\rho(\mathbf{r})], \quad (43)$$

where the full expressions for $A^{\mathrm{hs}}[\rho(\mathbf{r})]$ [Eq. (29)], $A^{\mathrm{chain}}[\rho(\mathbf{r})]$ [Eq. (30)], $A^{\mathrm{assoc}}[\rho(\mathbf{r})]$ [Eq. (31)], and $A_2[\rho(\mathbf{r})]$ [Eq. (35)] are used. The contribution due to the short-range part of the correlations in the attractive term is contained in $A_1^{\mathrm{sr}}[\rho(\mathbf{r})]$, which is defined in terms of the bulk term a_1^{sr} [Eq. (14)]. As this represents a short-range interaction it can be treated locally as

$$A_1^{\mathrm{sr}}[\rho(\mathbf{r})]=k_BT\int \mathrm{d}\mathbf{r}\, f_1^{\mathrm{sr}}(\rho(\mathbf{r}))$$

$$=k_BT\int \mathrm{d}\mathbf{r}\,\rho(\mathbf{r})ma_1^{\mathrm{sr}}(\rho(\mathbf{r})). \tag{44}$$

The mean-field dispersive term $A_{\mathrm{VR,mf}}^{\mathrm{att}}[\rho(\mathbf{r})]$ is described at the level of the van der Waals mean-field approximation in which the correlations due to attractive interactions are neglected. By making the approximation $g^{\mathrm{hs}}[\mathbf{r},\mathbf{r}';\rho(\mathbf{r}),\rho(\mathbf{r}')]=1$ in Eq. (38), the attractive term can be written in the familiar mean-field form as

$$A_{\mathrm{VR,mf}}^{\mathrm{att}}[\rho(\mathbf{r})]=\frac{1}{2}\int \mathrm{d}\mathbf{r}\, m\rho(\mathbf{r})\int \mathrm{d}\mathbf{r}'\, m\rho(\mathbf{r}')\phi^{\mathrm{att}}(|\mathbf{r}-\mathbf{r}'|). \tag{45}$$

This is the form of the attractive free energy functional used in our previous mean-field SAFT-HS DFT;[26,34] note that the factor of m^2 was omitted in error from Eq. (5) of Ref. 26. In contrast, however, the full free energy given by Eq. (42) reduces to the bulk SAFT-VR expression defined in Eq. (3) for a homogeneous system [at constant density $\rho(\mathbf{r})=\rho_{\mathrm{bulk}}$].

The Euler-Lagrange equation for the equilibrium profile in the case of the SAFT-VR MF DFT is now simply given by

$$\mu=\mu^{\mathrm{ideal}}(\rho(\mathbf{r}))+\mu_{\mathrm{VR,mf}}^{\mathrm{ref}}(\rho(\mathbf{r}))$$

$$+\int \mathrm{d}\mathbf{r}'\, m^2\rho(\mathbf{r}')\phi^{\mathrm{att}}(|\mathbf{r}-\mathbf{r}'|). \tag{46}$$

This expression is clearly obtained as a limiting form of Eq. (41) with $g^{\mathrm{hs}}(\sigma;\overline{\rho}_{\mathrm{eff}})=1$.

3. SAFT-HS MF DFT

In the SAFT-HS MF DFT approach both the bulk and the interfacial properties are treated at the mean-field level as far as the attractive forces are concerned. The SAFT-HS free energy functional was described in detail in previous work[26,34]; note that the expressions for the various contributions were not given consistently in terms of the density of spherical segments or that of molecules (e.g., see the corrected form of the hard-sphere [Eq. (29)] and chain [Eq. (30)] contributions). In our current notation the SAFT-HS Helmholtz free energy functional is represented by

$$A_{\mathrm{mf}}^{\mathrm{SAFT\text{-}HS}}[\rho(\mathbf{r})]=A^{\mathrm{ideal}}[\rho(\mathbf{r})]+A_{\mathrm{HS,mf}}^{\mathrm{ref}}[\rho(\mathbf{r})]$$

$$+A_{\mathrm{HS,mf}}^{\mathrm{att}}[\rho(\mathbf{r})], \tag{47}$$

where $A^{\mathrm{ideal}}[\rho(\mathbf{r})]$ is given by Eq. (27) and the local term $A_{\mathrm{HS,mf}}^{\mathrm{ref}}[\rho(\mathbf{r})]$ is now given by

$$A_{\mathrm{HS,mf}}^{\mathrm{ref}}[\rho(\mathbf{r})]=A^{\mathrm{hs}}[\rho(\mathbf{r})]+A^{\mathrm{chain}}[\rho(\mathbf{r})]+A^{\mathrm{assoc}}[\rho(\mathbf{r})], \tag{48}$$

in which the pair radial distribution function of the monomer fluid appearing in the expressions for $A^{\mathrm{chain}}[\rho(\mathbf{r})]$ [Eq. (30)] and $A^{\mathrm{assoc}}[\rho(\mathbf{r})]$ [Eq. (31)] is approximated by that of the hard-sphere reference $g^{\mathrm{sw}}[\sigma;\rho(\mathbf{r})]\approx g^{\mathrm{hs}}[\sigma;\rho(\mathbf{r})]$. The mean-field term $A_{\mathrm{HS,mf}}^{\mathrm{att}}[\rho(\mathbf{r})]$ is given by the van der Waals expression for inhomogeneous systems defined by Eq. (45), and the corresponding Euler-Lagrange equation is equivalent to Eq. (46).

C. The equilibrium density profile and surface tension

The equilibrium density profile is the profile for which the Euler-Lagrange condition, Eq. (25), holds at every point $\mathbf{r}$. In this study we examine a planar vapor-liquid interface where the density is a function of the position normal to the interface. Assuming that the interface is perpendicular to the z axis, the density profile depends only on the distance to the interface, i.e., $\rho(\mathbf{r})\equiv\rho(z)$. The Euler-Lagrange equation is underspecified as any translation of the equilibrium density profile in the z direction is also a solution of Eq. (25). A unique solution is assured by specifying that $z_{\max}$ and $z_{\min}$ be the boundary values equivalent to the coexistence bulk density of the liquid and vapor phases, respectively. In order to achieve an accurate solution the region over which the density profile deviates from the vapor and liquid bulk densities (interfacial thickness) must be narrower than the interval over which Eq. (25) is solved. The integration region ranges from $|z_{\max}-z_{\min}|\sim 2\sigma$ for states at a temperature $T\sim T_c/2$ (where T_c is the critical temperature) to $|z_{\max}-z_{\min}|\sim 15\sigma$ at $0.98\,T_c$. The integration in the z direction is performed numerically by selecting the range from $z_{\min}$ to $z_{\max}$ over which to integrate, and the interval is discretized into a large number of points z_i (typically 200 grid points *per* σ). A numerical integration of Eq. (25) is then performed by starting from a trial density profile ρ_{old} with limiting densities $\rho(z_{\max})$ and $\rho(z_{\min})$ which correspond to the vapor and liquid equilibrium bulk densities (the initial profile could be represented by a step profile), and solving the Euler-Lagrange equation numerically at each point z_i. This results in a new density profile ρ_{new} and the process is repeated until the density at each point z_i changes by no more than a specified tolerance.

Once the equilibrium density profile ρ_{eq} is known, the surface tension may be determined from the simple thermodynamic identity

$$\gamma=\frac{\Omega+PV}{\mathcal{A}}, \tag{49}$$

where $\mathcal{A}$ is the interfacial area and P is the bulk pressure.

III. RESULTS AND DISCUSSION

We apply the SAFT-VR DFT approach outlined in the preceding section to study the vapor-liquid interfacial properties of square-well fluids for various ranges of the potential, molecular chains of square-well segments, and associating fluids with different association schemes. Before studying the vapor-liquid interface, we use the bulk SAFT-VR equation of state to determine the vapor-liquid equilibrum by solving the equilibrium conditions, i.e., the equality of pressure and chemical potential in the vapor and liquid phases. In what follows, the attractive interaction parameter ε is chosen as the unit of energy and the hard-sphere diameter σ as the unit of length. According to this, we define the following reduced quantities: temperature, $T^*=k_BT/\varepsilon$; density, $\rho^*=\rho\sigma^3$; surface tension, $\gamma^*=\gamma\sigma^2/\varepsilon$; distance from the interface, $z^*=z/\sigma$; strength of the site-site association interaction, $\varepsilon_{hb}^*=\varepsilon_{hb}/\varepsilon$; and bonding volume, $K_{hb}^*=K_{hb}/\sigma^3$.

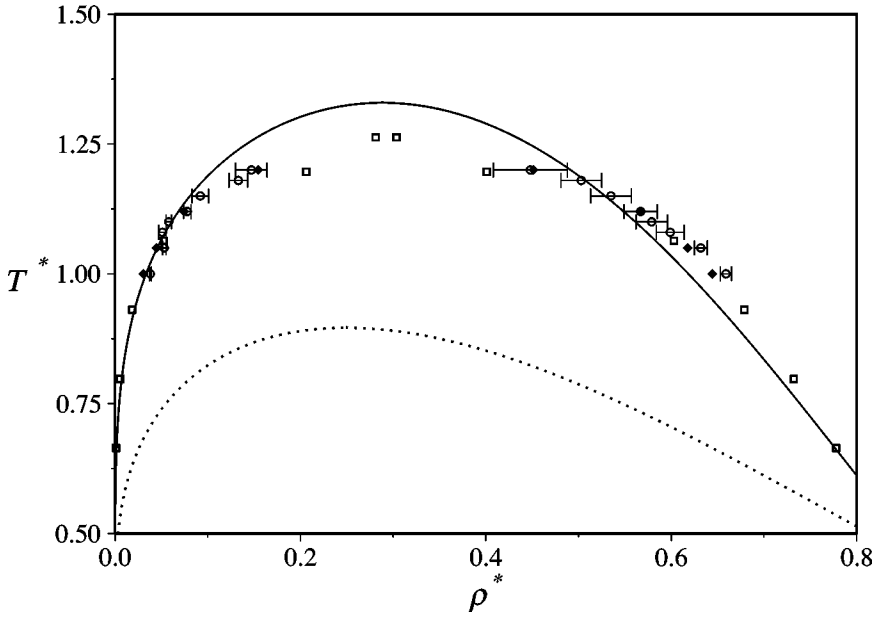

FIG. 1. The vapor-liquid coexistence curve for the square-well fluid of range $\lambda = 1.5$, where $T^* = k_B T/\varepsilon$ and $\rho^* = \rho\sigma^3$ are the reduced temperature and number density, respectively. The points correspond to Monte Carlo simulation data: white circles with error bars, Vega *et al.* (Ref. 85); black diamonds, del Rio *et al.* (Ref. 86); squares, Gloor *et al.* (Refs. 70 and 71). The predictions of the SAFT-VR approach [Eq. (3)] are represented by the continuous curve, while those of the mean-field SAFT-HS approach (Refs. 35 and 37) are represented by the dotted curve.

The mean-field version of the SAFT theory (SAFT-HS) presented in the previous papers[26,34] can be used to describe the vapor-liquid interfacial tension of a wide variety of fluids. A good description of the temperature dependence of the surface tension was, however, only achieved after using the range of the intermolecular potential as an adjustable parameter. Though this is perfectly valid as an engineering tool, the predictive nature of the theory is thus limited.

A mean-field approach is not generally expected to provide a quantitative description of the vapor-liquid properties for a system with realistic interactions (see, Refs. 23, 24, and 47). This is illustrated in Fig. 1 for a square-well fluid of range $\lambda = 1.5$, where the SAFT-HS (mean-field) and SAFT-VR (perturbation expansion) predictions are compared with simulation data.[70,71,85,86] The recent simulation data[70,71] were obtained from a test area Monte Carlo simulation of the system with an interface and extends the range of the data to lower temperatures than those accessible with the Gibbs ensemble Monte Carlo (GEMC) technique.[85] Clearly the mean-field SAFT-HS approach underestimates the saturated liquid density (the whole coexistence envelop is shifted downwards). The SAFT-VR description of the liquid density is much more accurate, though it is seen to slightly overestimate the critical temperature. The mean-field (SAFT-HS) approach also fails in predicting accurate density profiles. This is shown in Fig. 2 for a square-well system at temperature $T^* = 0.798$. The profiles obtained with SAFT-HS are broader than those obtained with SAFT-VR, and do not provide an accurate representation of the simulation data; as seen in Fig. 1, the mean-field profile does not yield accurate limiting coexisting densities (particularly that of the liquid). As expected DFTs based on the mean-field SAFT-HS approach are not recommended for quantitative predictions.

We have used two approaches to construct a SAFT-VR DFT which incorporates correlations in the attractive contributions (see Secs. II B 1 and II B 2): in the SAFT-VR MF DFT approach of Sec. II B 2, correlations are removed from the perturbative term and the reference term is corrected to yield the homogeneous limit [cf. Eq. (42)]; in the full SAFT-VR DFT approach of Sec. II B 1, the average correlations are retained at first-order level in the perturbative term [cf. Eq. (26)]. There is only a small difference between these two approaches as far as the interfacial profiles are concerned, with a slightly better description when correlations are included in the perturbative term (see Fig. 2). It is important to note that both approximations provide the same bulk phase behavior and limiting coexistence densities. However, after examining the surface tension, it becomes apparent that correlations should be incorporated to provide the best description. The vapor-liquid surface tension data obtained from molecular simulation using the thermodynamic[70,71,87] and mechanical[87,88] approaches for a square-well fluid with a range of $\lambda = 1.5$ are compared with the various versions of the SAFT DFT in Fig. 3. The data for the surface tension obtained with the new test area method[70,71] are seen to be consistent with the existing data. In line with our previous comments, the corresponding values obtained from the mean-field SAFT-HS approach deviate significantly from the simulation results (see the paper by Winkelmann[15] for a similar analysis). The SAFT-VR MF DFT mean-field approach provides a better description of the surface tension for temperatures approaching the critical point, though the results are seen to deviate from the simulation data at lower temperatures. The incorporation of correlations in the perturbative term (SAFT-VR DFT approach) greatly improves the theoretical description of the surface tension at lower temperatures. The description of the surface tension with the SAFT-VR DFTs is consistent with the description of the

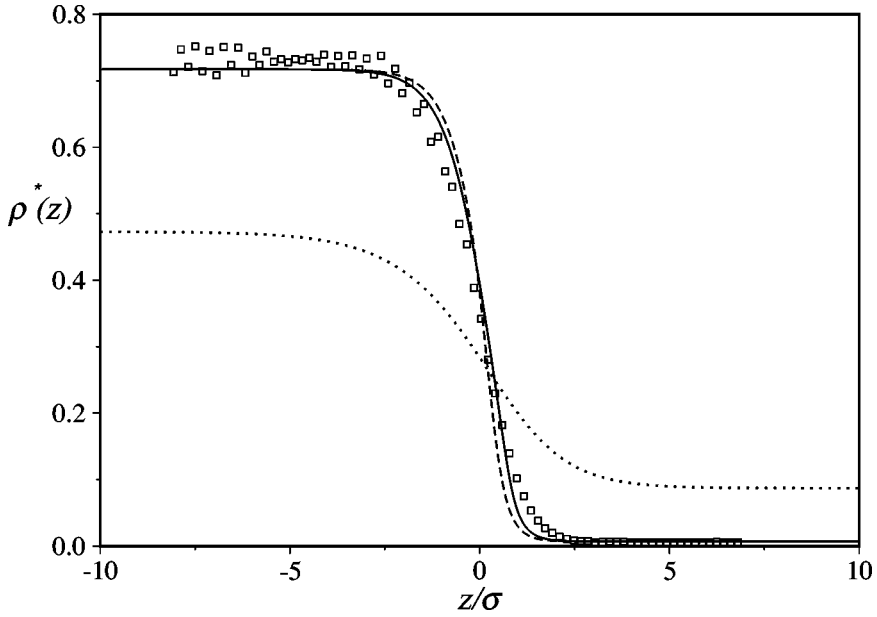

FIG. 2. The vapor-liquid density profile $\rho^*(z)=\rho(z)\sigma^3$ as a function of the distance from the interface $z^*=z/\sigma$ for the square-well fluid of range $\lambda=1.5$ for a reduced temperature $T^*=0.798$. The results obtained from the direct Monte Carlo simulation of the inhomogeneous system (Refs. 70 and 71) are denoted as the squares. The predictions of the various density functional theories are included for comparison: full SAFT-VR DFT [Eq. (26)], continuous curve; mean-field SAFT-VR MF DFT [Eq. (42)], dashed curve; and mean-field SAFT-HS MF DFT [Eq. (47)], dotted curve.

vapor-liquid equilibria: the theory fails by slightly overpredicting the critical temperature of the system. In the remaining discussion we assess the adequacy of the full SAFT-VR DFT approach [cf. Eq. (26)] in describing the surface tension of various systems.

The SAFT-VR equation of state, which is essentially a second-order Barker-Henderson perturbation approach, provides a good description of the vapor-liquid fluid phase equilibria of square-well systems of variable range.[47] The coexistence envelope obtained with this approach for square-well systems with $\lambda=1.25$, 1.5, and 1.75 are compared with simulated values in Fig. 4(a). The coexisting liquid densities obtained from direct simulations of the inhomogeneous system with a range of $\lambda=1.75$ (Refs. 70 and 71) are slightly

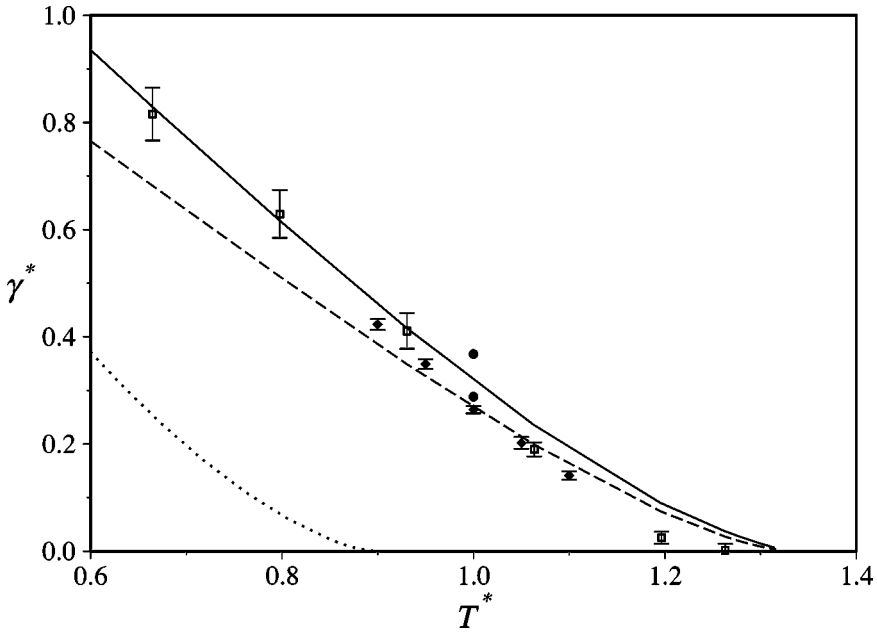

FIG. 3. The vapor-liquid surface tension $\gamma^*=\gamma\sigma^2/\varepsilon$ as a function of the temperature $T^*=k_BT/\varepsilon$ for the square-well fluid of range $\lambda=1.5$. The points correspond to molecular simulation data: black circles, Henderson and van Swol (Ref. 87); black diamonds with error bars, Orea *et al.* (Ref. 88); squares with error bars, Gloor *et al.* (Refs. 70 and 71). Note that the value of the surface tension obtained by Henderson and van Swol (Ref. 87) at the temperature $T^*=1$ for a confined system with a mechanical approach appears to be slightly too large (upper black circle). The predictions of the various density functional theories are included for comparison: full SAFT-VR DFT [Eq. (26)], continuous curve; mean-field SAFT-VR MF DFT [Eq. (42)], dashed curve; and mean-field SAFT-HS MF DFT [Eq. (47)], dotted curve.

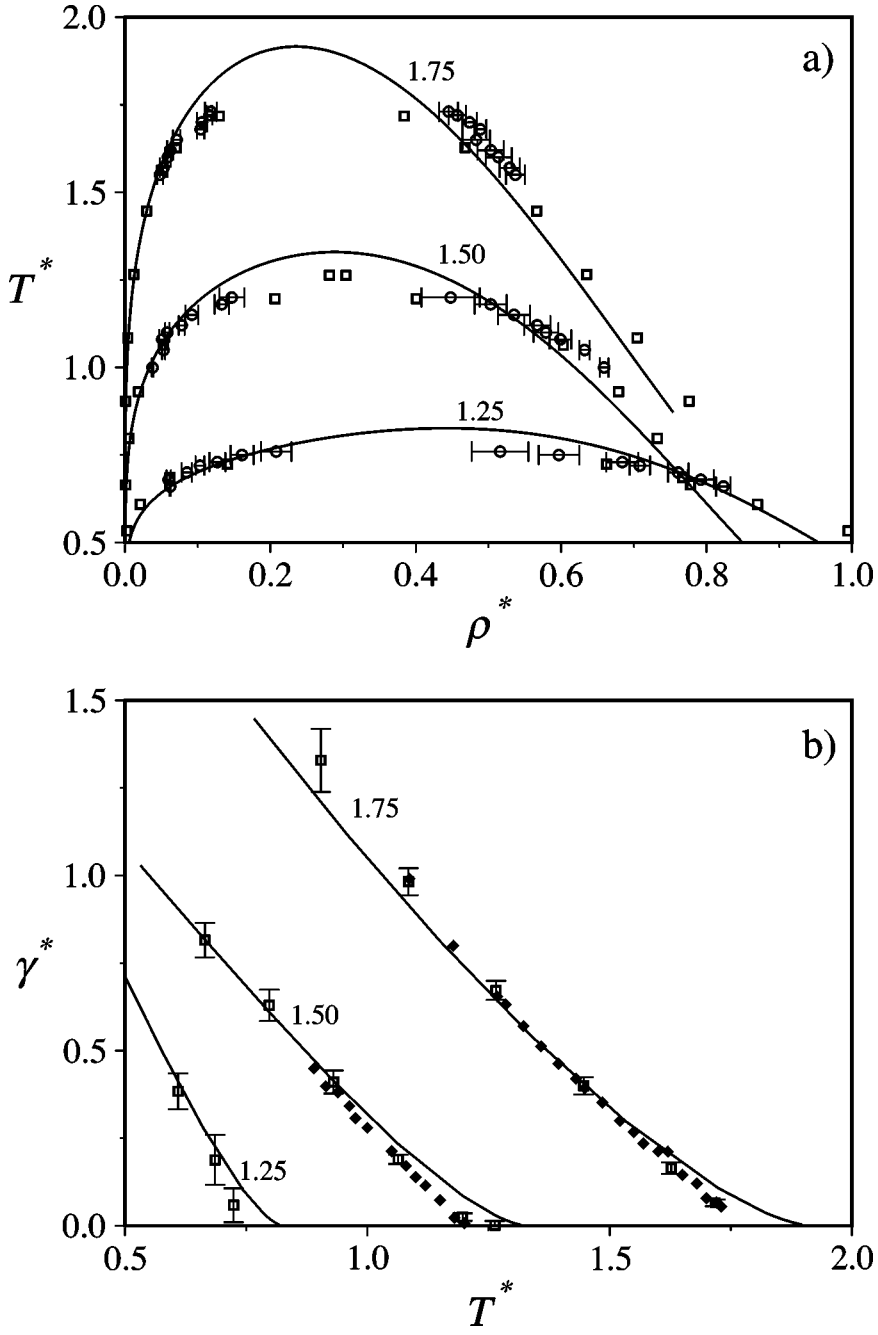

FIG. 4. (a) The vapor-liquid coexistence curve for the square-well fluid, where $T^*=k_BT/\varepsilon$ and $\rho^*=\rho\sigma^3$ are the reduced temperature and number density, respectively. The points correspond to Monte Carlo simulation data: circles with error bars, Vega *et al.* (Ref. 85); squares, Gloor *et al.* (Refs. 70 and 71). The predictions of the SAFT-VR approach [Eq. (3)] are represented by the continuous curves. The specific range of the interaction λ is denoted for each system. (b) The corresponding vapor-liquid surface tension $\gamma^*=\gamma\sigma^2/\varepsilon$ as a function of the reduced temperature. The points correspond to molecular simulation data: black diamonds, Singh *et al.* (Ref. 89); squares with error bars, Gloor *et al.* (Refs. 70 and 71). The continuous curves represent the predictions of the SAFT-VR DFT [Eq. (26)].

lower than the GEMC data,[85] probably due to a system size effect. The temperature dependence of the surface tension for the square-well fluid of variable range is shown in Fig. 4(b) (see Table I for a numerical comparison). The agreement between the SAFT-VR DFT predictions and the simulation data[70,71,89] is remarkable considering the wide range of λ values. A change in the slope of the surface tension is observable as the potential range is reduced. This suggests that the surface tension is a sensitive measure of the range of the interactions, a point that will be further emphasized after examining associating systems.

An expression for the thermodynamic properties of chain molecules can be obtained from the Wertheim[36,79] TPT1 approach in the limit of complete association; the contributions for chain formation and association in the SAFT-VR free energy are based on the Wertheim expressions. It is important to recall that in our current SAFT-VR DFT approach, the chain and association contributions are

TABLE I. The coexisting vapor $\rho_v^*=\rho_v\sigma^3$ and liquid $\rho_l^*=\rho_l\sigma^3$ densities and surface tension $\gamma^*=\gamma\sigma^2/\varepsilon$ for square-well fluids of range λ obtained from MC simulation at various temperatures $T^*=k_BT/\varepsilon$ (chosen to correspond roughly to the same relative distance from the critical temperature). The surface tensions γ_{MC}^* obtained from a test area Monte Carlo simulation method (Refs. 70 and 71) are compared with the predictions $\gamma_{\mathrm{SAFT\text{-}VR}}^*$ of the SAFT-VR DFT [Eq. (26)].

λ	T^*	ρ_l^*	ρ_v^*	γ_{MC}^*	$\gamma_{\mathrm{SAFT\text{-}VR}}^*$
1.25	0.6090	0.8699	0.0207	0.38 (5)	0.410
	0.6858	0.7670	0.0616	0.19 (7)	0.222
	0.7239	0.6623	0.1406	0.06 (5)	0.140
1.50	0.6647	0.7779	0.0010	0.82 (5)	0.817
	0.7977	0.7322	0.0056	0.63 (5)	0.610
	0.9306	0.6789	0.0186	0.41 (3)	0.413
	1.064	0.6030	0.0527	0.190 (13)	0.234
	1.196	0.4009	0.2063	0.025 (11)	0.0856
	1.263	0.3036	0.2812	0.002 (12)	0.0306
1.75	0.9040	0.7758	0.0007	1.33 (9)	1.21
	1.084	0.7045	0.0038	0.98 (4)	0.913
	1.265	0.6350	0.0121	0.67 (3)	0.643
	1.446	0.5663	0.0297	0.40 (3)	0.402
	1.627	0.4676	0.0704	0.164 (16)	0.197
	1.718	0.3840	0.1297	0.066 (9)	0.113

included in the reference term of the free energy functional. The vapor-liquid bulk coexistence densities for flexible chains formed from $m=4$ and 8 tangent square-well segments of range $\lambda=1.5$ obtained from the SAFT-VR equation of state and Monte Carlo simulation[90] are depicted in Fig. 5(a); the results for $m=1$ (square-well monomers) are also included in the figure for comparison. As it has been shown in previous work,[47] good agreement between the theory and simulation data is found. The critical temperature is seen to increase with increasing chain length, accompanied by a corresponding narrowing of the density envelope. The effect of increasing the chain length on the surface tension is shown in Fig. 5(b). The surface tension curves are shifted to higher temperatures when the chain length is increased as was found with the SAFT-HS DFT approach.[26] The limiting curve of infinitely long chains is difficult to obtain because the saturation pressure and density of the coexisting vapor phase are very low for this system. We have instead determined the vapor-liquid critical temperature T_c for infinitely long chains and assumed a Guggenheim[11,91] corresponding-states law $\gamma=\gamma_0(1-T/T_c)^{1.23}$. The zero-temperature surface tension γ_0 was found to be practically constant ($\gamma_0=1.9$ to within 1%) for systems with chain lengths of $m=1$ to 10; this value was used to estimate $\gamma(T)$ in the limit $m\to\infty$. Similar Wertheim DFT schemes have been used within a WDA to study the free surfaces of long chain molecules.[31,80–82]

We now turn to a detailed examination of the effect of association on the surface tension for a number of model systems. The first model is a dimerizing system of spherical molecules; this corresponds to a molecule with a single bonding site which is allowed to bond to a free site on another molecule (model 1). A one-site model of the type described here can be used to represent the dimerization equilibria behavior exhibited by real systems such as carboxylic acids; the thermodynamic properties of acetic acid are well known to be dominated by a dimerization equilibria. Borowko *et al.*,[29] Peery and Evans,[32] and more recently Alejandre *et al.*[33] have studied this model using a mean-field Wertheim DFT (cf. SAFT-HS MF DFT). A broadening of the density profile on dimerization is found, as well as a shift of the profile of unbonded molecules towards the vapor side of the interface (also see Ref. 26); a related (slight) peak in the density of unbonded molecules close to the interface has also been reported.[33] The vapor-liquid coexistence densities of a dimerizing square-well fluid (model 1) with range $\lambda=1.5$ obtained from the SAFT-VR theory is depicted in Fig. 6(a) for strengths of the site-site association interaction ranging from the non-associating limit ($\varepsilon_{hb}=0$) to the fully dimerized fluid ($\varepsilon_{hb}=\infty$). It is clear that for the one-site model the fluid-phase equilibria is bounded by these two limiting cases. This is also true for the temperature dependence of the surface tension [see Fig. 6(b)]. In the case of the system with an association site-site interaction energy of intermediate strength ($\varepsilon_{hb}^*=8$) and a relatively small bonding volume of $K_{hb}^*=0.001$ (corresponding to $r_d^*=0.25$ and $r_c^*=0.5606$) the surface tension varies from values corresponding to the fully dimerized system at low temperatures to those of the nonassociated system as the temperature is increased towards the critical point. This provides a simple interpretation for the characteristic *s* shaped curve seen in some associating compounds such as water or alcohols.[11] As expected the surface tension always increases with increasing association. A misleading interpretation of the effect of association can be made when the temperature is reduced by the critical temperature, as the surface tension may appear to decrease when the degree of association is increased (see Fig. 4 of both Refs. 26 and 32). For a relatively weak association energy [see the curve for $\varepsilon_{hb}^*=4$ in Fig. 6(b)] the surface tension increases slightly with decreasing temperature when compared to the nonassociating system. In the case of a strong site-site interaction [$\varepsilon_{hb}^*=16$ in Fig. 6(b)] the surface tension has essentially saturated to the corresponding value of the fully dimerized system, and the temperature dependence resembles that of the nonassociating dimer. The particular behavior of $\gamma(T)$ is also very sensitive to the range of the association interaction (bonding volume). The surface tension for the single site square-well fluid with a larger bonding volume of $K_{hb}^*=0.1$ (corresponding to $r_d^*=0.25$ and $r_c^*=0.7631$) is also shown in Fig. 6(b). In this case the *s*-shaped behavior is found to be less dramatic than for the system with the smaller bonding volume, and the temperature dependence is very similar to that of a nonassociating system (with the curves shifted to higher temperatures). The reason for this is that for large bonding volumes the system remains dimerized over almost the entire temperature range even for moderate association energies. The sharp change in association for the system with a large energy and small bonding volume produces a marked change in curvature. It is also interesting to point out that although the systems with $\varepsilon_{hb}^*=16$ and $K_{hb}^*=0.001$ and with $\varepsilon_{hb}^*=8$ and $K_{hb}^*=0.1$ have very similar critical points and low-temperature surface tensions, a marked difference in surface tension and curva-

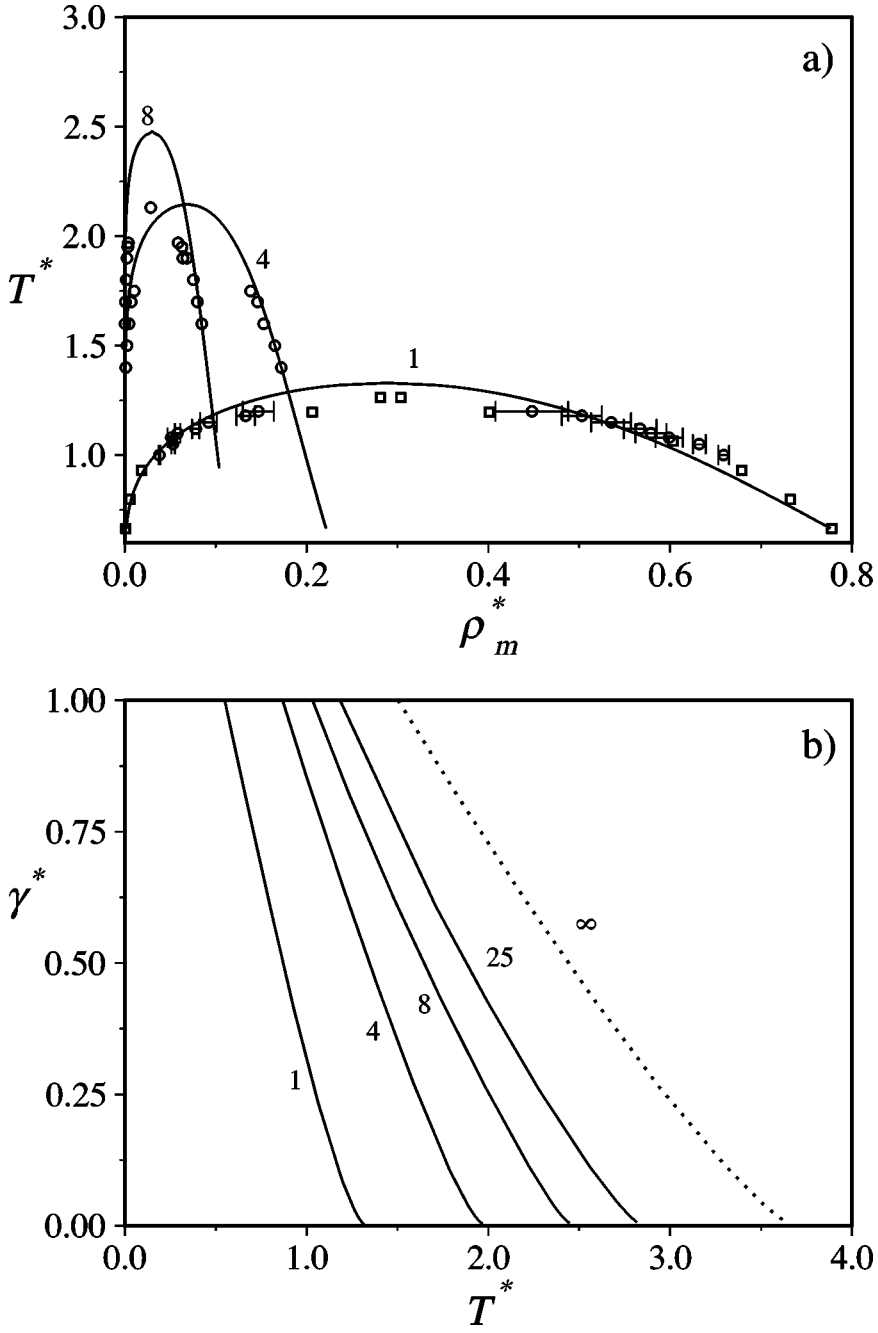

FIG. 5. (a) The vapor-liquid coexistence curve for chains formed from m tangent square-well segments, where $T^*=k_BT/\varepsilon$ and $\rho_m^*=\rho\sigma^3$ are the reduced temperature and number density of chain molecules, respectively. The points correspond to Monte Carlo simulation data: for $m=4$ and 8, Escobedo and de Pablo (Ref. 90); for $m=1$, Vega *et al.* (Ref. 85) (circles) and Gloor *et al.* (Refs. 70 and 71) (squares). The predictions of the SAFT-VR approach [Eq. (3)] are represented by the continuous curves. (b) The corresponding vapor-liquid surface tension $\gamma^*=\gamma\sigma^2/\varepsilon$ as a function of the reduced temperature. The continuous curves represent the predictions of the SAFT-VR DFT [Eq. (26)]; the limit for the infinitely long chain ($m=\infty$) is shown as the dotted curve.

ture is seen for intermediate temperatures. This suggests that the surface tension does not generally follow the Guggenheim scaling relation in the case of dimerizing systems. By contrast, the vapor-liquid coexistence curves for these two systems are very similar [see Fig. 6(a)], and conform to a corresponding states law. This has important implications in obtaining optimal parameters for the description of the vapor-liquid equilibria and surface tension for real compounds.[70,92]

In order to assess the adequacy of our SAFT-VR DFT in describing the vapor-liquid interface of dimerizing fluids we also compare our theoretical predictions with the very recent simulation data of Singh and Kofke[46] for a one-site square-well fluid. The specific model studied by Singh and Kofke incorporates a conical square-well bonding site of range r_c^* and angular cutoff θ_c on an isotropic square well; in this case the bonding volume is defined as $K_{hb}^*=\pi(1-\cos\theta_c)^2(r_c^*-1)$.[35] The values for the surface tension obtained from the simulations for association energies of $\varepsilon_{hb}^*=4$ and 7 and a bonding volume of $K_{hb}^*=0.001\,866$ (corresponding to $r_c^*=1.05$ and $\theta_c=27°$) are compared with the predictions of our SAFT-VR DFT in Fig. 7. As was found for the nonasso-

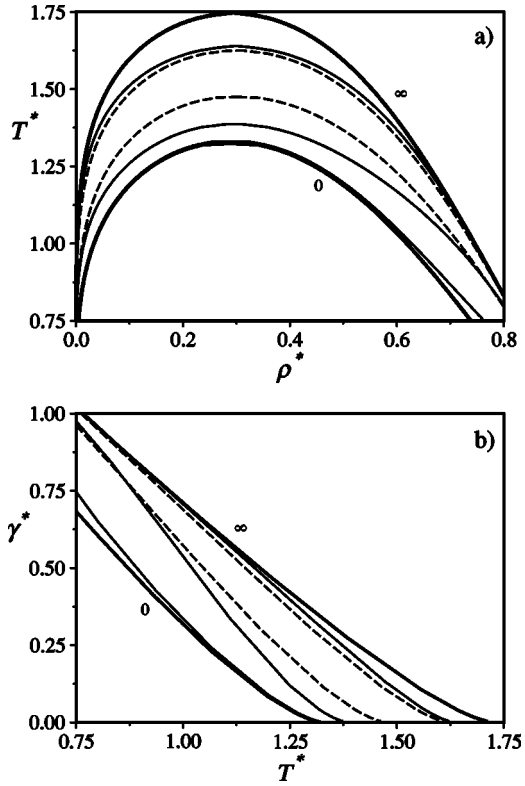

FIG. 6. (a) The vapor-liquid coexistence curve for a single-site associating (dimerising) square-well fluid (model 1 in the discussion), where $T^* = k_B T/\varepsilon$ and $\rho^* = \rho\sigma^3$ are the reduced temperature and number density, respectively. The predictions of the SAFT-VR approach [Eq. (3)] are represented by the curves: the continuous curves correspond to a small bonding volume of $K_{hb}^* = 0.001$ (with $r_d^* = 0.25$ and $r_c^* = 0.5606$), and the dashed curves to a large bonding volume of $K_{hb}^* = 0.1$ (with $r_d^* = 0.25$ and $r_c^* = 0.7631$). The site-site bonding interaction is $\varepsilon_{hb}^* = 4$, 8, and 16 (curves from top to bottom); the limiting cases of the nonassociating ($\varepsilon_{hb}^* = 0$) and fully associated dimer ($\varepsilon_{hb}^* = \infty$) systems are also shown as the thick continuous curves for reference. The curves for the system with the strongest bonding interactions ($K_{hb}^* = 0.1$ and $\varepsilon_{hb}^* = 16$) are indistinguishable from those of the fully associated system. (b) The corresponding vapor-liquid surface tension $\gamma^* = \gamma\sigma^2/\varepsilon$ as a function of the reduced temperature. The curves represent the predictions of the SAFT-VR DFT [Eq. (26)]; see part a for details of the various systems.

ciating square-well system (see Fig. 3), the theory slightly overestimates the simulation data for the surface tension of the associating system at the higher temperatures, essentially because of an overestimate of the critical temperature. At lower temperatures the agreement is expected to improve, as is found for the nonassociating fluid [cf. Figs. 3 and 4(b)], but unfortunately the simulations for the associating system were not carried out at low enough temperatures for us to assess this. The surface tension of the system with $\varepsilon_{hb}^* = 4$ is only slightly larger than that of the nonassociating system; for a site-site association energy of $\varepsilon_{hb}^* = 7$ there is an appreciable increase in the surface tension due to dimerisation. It is difficult to make any claims about the curvature of $\gamma(T)$ again because of the relatively small temperature range considered in the simulations. According to the theoretical predictions for the dimerizing systems studied by Singh and Kofke, an *s*-shaped behavior is not expected for this specific choice of the association energy and bonding volume.

The next prototype model of association that deserves particular attention is the two-site model, where only unlike association is permitted (we refer to this as the 1:1 model). The two sites, labeled *A* and *B*, are allowed to form *A*-*B* bonds, but no *A*-*A* or *B*-*B* association is permitted. In this case, chainlike aggregates can form in the fluid, and the limit of complete association corresponds to a single infinitely long ''polymer'' chain. This type of model can be used to represent the aggregation in a system of highly dipolar molecules such as hydrogen fluoride[57] or alcohols[93–95] (when only one of the lone pairs on the oxygen atom is assumed to be involved in the hydrogen bonding). The vapor-liquid coexistence curves of the two-site square-well system (model 1:1) with $\lambda = 1.5$ are depicted in Fig. 8(a) for site-site association energies of $\varepsilon_{hb}^* = 2$, 4, and 8, and a relatively small bonding volume of $K_{hb}^* = 0.001$ (corresponding to $r_d^* = 0.25$ and a range $r_c^* = 0.5606$). The coexistence curve in the limit of complete association corresponding to an infinitely long chain has not been included in the figure due to the large difference in scale (see the related papers by Vega and MacDowell[96] and Blas *et al.*[97]). As the degree of association is increased, the coexistence envelopes shift to higher temperatures. The effect of association on the surface tension of the 1:1 model is shown in Fig. 8(b). The temperature dependence that is obtained is similar to that found for the one-site system [cf. Fig. 6(b)]: for weak association energies ($\varepsilon_{hb}^* = 2$) the surface tension is only slightly higher than that of the nonassociating fluid and the difference increases slightly as the temperature is lowered; for a system with a large association energy ($\varepsilon_{hb}^* = 8$) and a relatively small bonding volume ($K_{hb}^* = 0.001$), the surface tension displays the characteristic *s*-shaped temperature dependence as it tends from the fully associated limit at low temperatures to the nonassociated limit at higher temperatures. The main difference is that the surface tension does not saturate as rapidly to the fully associated limit for the two-site model as it does for the corresponding one-site model. This is expected when one considers that much more energy is required to form a fully associated infinite chain than a fully associated dimer. For systems with the larger bonding volume ($K_{hb}^* = 0.1$), there is a larger increase in the surface tension from that of the nonassociated system than for systems with the smaller bonding volumes ($K_{hb}^* = 0.001$). Systems with larger bonding volumes also exhibit less curvature in the temperature dependence of the surface tension, so that the curves obtained for different values of the association energy appear more parallel than the corresponding curves for systems with smaller bonding volumes. A similar temperature dependence of the surface tension for the two-site associating system was reported with the mean-field SAFT-HS MF DFT,[26] where an additional analysis of the effect of association on the average aggregate size was made. A mean-field DFT based on the Wertheim theory of association was also used by Pizio *et al.*[31] to examine the effect of confinement on a fluid of two-site associating Lennard-Jones molecules. In their case, however, the site-site association energy was kept fixed and the effect of varying the pore size and strength of the particle-wall interaction was studied.

A three-site model can be used to represent an association scheme which involves the formation of branched as

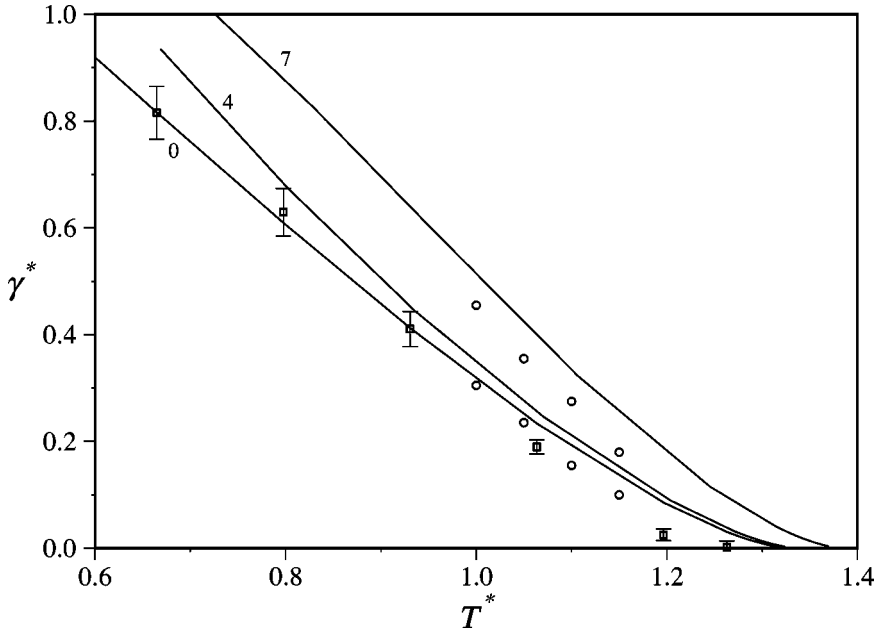

FIG. 7. The vapor-liquid surface tension $\gamma^* = \gamma\sigma^2/\varepsilon$ as a function of the temperature $T^* = k_B T/\varepsilon$ for a single-site associating (dimerizing) square-well fluid (model 1). The points correspond to molecular simulation data: circles, Singh and Kofke;[46] squares with error bars, Gloor *et al.* (Refs. 70 and 71). The curves represent the predictions of the SAFT-VR DFT [Eq. (26)]. In this case the bonding volume is $K_{hb}^* = 0.001\,866$ and site-site bonding energies of $\varepsilon_{hb}^* = 0$, 4, and 7 are considered.

well as chainlike aggregates. Here, we examine a three-site model in which two sites are equivalent (model 1:2); one site is labeled *A*, the two remaining sites are labeled *B*, and only *A*-*B* bonding is allowed. Hydrogen bonding between the two lone pairs on the oxygen and the hydrogen of a hydroxyl group could be represented in such a way (e.g., see Refs. 93 and 94); in some cases, however, steric effects (such as those present in long-chain alcohols) prevent all three sites to be involved in the bonding, and a two-site model is preferable. The vapor-liquid equilibria and surface tension of model 1:2 is depicted in Fig. 9 for systems with different site-site association energies ($\varepsilon_{hb}^* = 2$, 4 and 8), and bonding volumes ($K_{hb}^* = 0.001$ and $K_{hb}^* = 0.1$). As in the previous models, the two-phase vapor-liquid region extends to higher densities and temperatures with increasing association, the effect becoming more pronounced for the systems with the larger bonding volume of $K_{hb}^* = 0.1$ [see Fig. 9(a)]. For systems with a smaller bonding volume of $K_{hb}^* = 0.001$ (corresponding to $r_d^* = 0.25$ and $r_c^* = 0.5606$) $\gamma(T)$ appears to exhibit more curvature for the three-site model than for the corresponding curves of the two-site model [cf. Fig. 8(b)]; this feature turns out to be important in describing the surface tension of the shorter chain alkanols such as propan-2-ol.[92] Interestingly, the surface tension curves all appear to be within the upper bound corresponding to the infinitely long chain; the number of bonds in the limit of infinite association for the 1:2 model is the same as that of the two-site infinite chain (1:1 model). The TPT1 approach of Wertheim[36,79] cannot be used to distinguish between different isomers of a given chain (also see Ref. 98), and so does not differentiate between different branched structures. This is also true for the asymmetric 1:3 four-site model, but not for the symmetric 2:2 model which can form an aggregated network structure, as is discussed in the following paragraph.

We now examine two prototype four-site association models. In the first (asymmetric 1:3 model), three of the four sites are equivalent; one site is labeled *A* and the rest *B*, and again only *A*-*B* bonding is allowed. The 1:3 model can be used to describe the vapor-liquid equilibria and surface tension of molecules such as ammonia.[92,94] Predictions for this model of branched association are shown in Fig. 10. Upon comparison with Fig. 9, both the 1:3 and 1:2 models display similar qualitative features. The surface tension curves of the 1:3 model are again bounded by the limiting curve for the infinitely long chain, as the number of bonds of asymmetric 1:3 systems in the limit of complete association is the same as that of the infinitely long chain (1:1 model). The symmetric four-site 2:2 model is frequently used to model water, where two sites represent the hydrogen atoms and the other two represent the lone pairs on the oxygen atom (e.g., see Refs. 37, 54, 93, 99–101). The model now has two pairs of equivalent sites; one pair is labeled *A*, the other *B*, and only *A*-*B* bonding is allowed. Because of the greater possibilities for bonding in such a network structure, the effect of association on the coexistence curve is expected to be quite significant, particularly for systems with a large bonding volume. The coexistence and surface tension curves for the 2:2 model are depicted in Fig. 11. This model is seen to exhibit a qualitatively different surface tension behavior than the other models examined thus far. Unlike the other models, where the surface tension has an upper bound corresponding to the limit of an infinitely long polymer chain, the 2:2 model is characterized by large surface tensions. The increase in association and surface tension with decreasing temperature is very dramatic. At the lower temperatures the surface tension is not constrained to be lower than that of infinite chain limit (1:1 model), because the 2:2 model can now form complex networks in the limit of full association. In this limit the

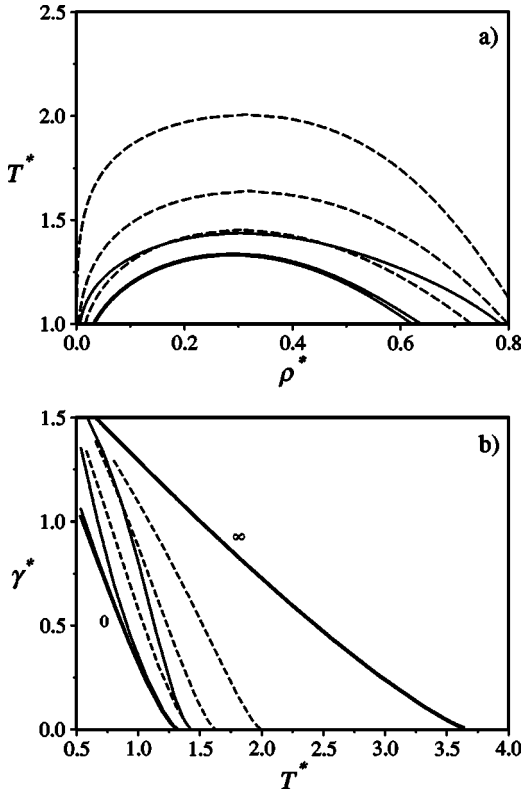

FIG. 8. (a) The vapor-liquid coexistence curve for a two-site associating (chain forming) square-well fluid (model 1:1), where $T^*=k_BT/\varepsilon$ and $\rho^*=\rho\sigma^3$ are the reduced temperature and number density, respectively. The predictions of the SAFT-VR approach [Eq. (3)] are represented by the curves: the continuous curves correspond to a small bonding volume of $K^*_{hb}=0.001$ (with $r^*_d=0.25$ and $r^*_c=0.5606$), and the dashed curves to a large bonding volume of $K^*_{hb}=0.1$ (with $r^*_d=0.25$ and $r^*_c=0.7631$). The site-site bonding interaction is $\varepsilon^*_{hb}=2$, 4 and 8 (curves from top to bottom). (b) The corresponding vapor-liquid surface tension $\gamma^*=\gamma\sigma^2/\varepsilon$ as a function of the reduced temperature. The curves represent the predictions of the SAFT-VR DFT [Eq. (26)]; see part a for details of the various systems. The limiting cases of the nonassociating ($\varepsilon^*_{hb}=0$) and fully associated dimer ($\varepsilon^*_{hb}=\infty$) systems are also shown as the thick continuous curves for reference.

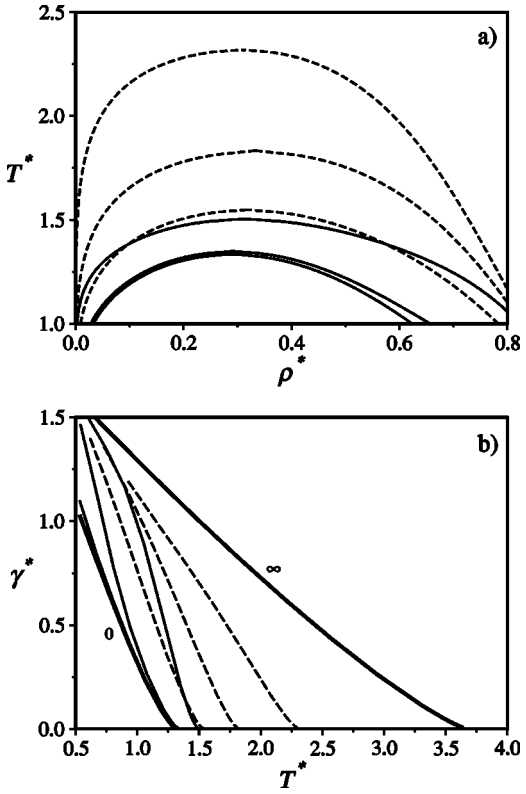

FIG. 9. (a) The vapor-liquid coexistence curve for a three-site associating (branched chain forming) square-well fluid (model 1:2), where $T^*=k_BT/\varepsilon$ and $\rho^*=\rho\sigma^3$ are the reduced temperature and number density, respectively. The predictions of the SAFT-VR approach [Eq. (3)] are represented by the curves: the continuous curves correspond to a small bonding volume of $K^*_{hb}=0.001$ (with $r^*_d=0.25$ and $r^*_c=0.5606$), and the dashed curves to a large bonding volume of $K^*_{hb}=0.1$ (with $r^*_d=0.25$ and $r^*_c=0.7631$). The site-site bonding interaction is $\varepsilon^*_{hb}=2$, 4, and 8 (curves from top to bottom). (b) The corresponding vapor-liquid surface tension $\gamma^*=\gamma\sigma^2/\varepsilon$ as a function of the reduced temperature. The curves represent the predictions of the SAFT-VR DFT [Eq. (26)]; see part a for details of the various systems. The limiting cases of the nonassociating ($\varepsilon^*_{hb}=0$) and fully associated dimer ($\varepsilon^*_{hb}=\infty$) systems are also shown as the thick continuous curves for reference.

average number of bonds per molecule in the 2:2 model is greater than for the other models, which in turn leads to a large cohesive energy and surface tension.

It is instructive to compare the surface tension curves for some of the models examined in the preceding discussion with more realistic values of the parameters (see Refs. 70 and 92 for details). The surface tension curves of ethane (nonassociating model), the refrigerant 1,1,1,2-tetrafluoroethane or R134a (chain forming two-site 1:1 model), ethanol (branched chain forming three-site 1:2 model), ammonia (branched chain forming four-site 1:3 model), and water (network forming 2:2 four-site model) obtained from the SAFT-VR DFT approach are presented in Fig. 12. The intermolecular potential parameters are optimized to provide the best description of the experimental vapor-liquid equilibria and surface tension data;[102,103] in the case of ethane the parameters obtained from vapor-liquid equilibria alone give a good description of the surface tension. As one would expect, the surface tension becomes progressively larger as the degree of molecular association in the system is increased from the nonassociating system (ethane) to the four-site associating system (water). Furthermore, the curvature of $\gamma(T)$ is very sensitive to the mechanism of association in the fluid. In the case of the nonassociating ethane system the curvature is always positive (concave up) and will conform to Guggenheim scaling; the slight departure of the theoretical description from the experimental data is due to an overprediction of the critical temperature (see Ref. 47). The curvature of the surface tension curve for ethanol (described with the three-site 1:2 model) is negative (concave down) for most of the fluid range. In the case of water (described with the four-site 2:2 model), the surface tension curve exhibits a clear point of inflection at intermediate temperatures where the curvature changes sign and the characteristic *s*-shaped behavior is seen. In all cases, the description of the experimental surface tension by the SAFT-VR DFT is very good considering the fundamental differences in the molecular interactions of the systems involved. A more detailed examination of the adequacy of the approach in describing the interfacial proper-

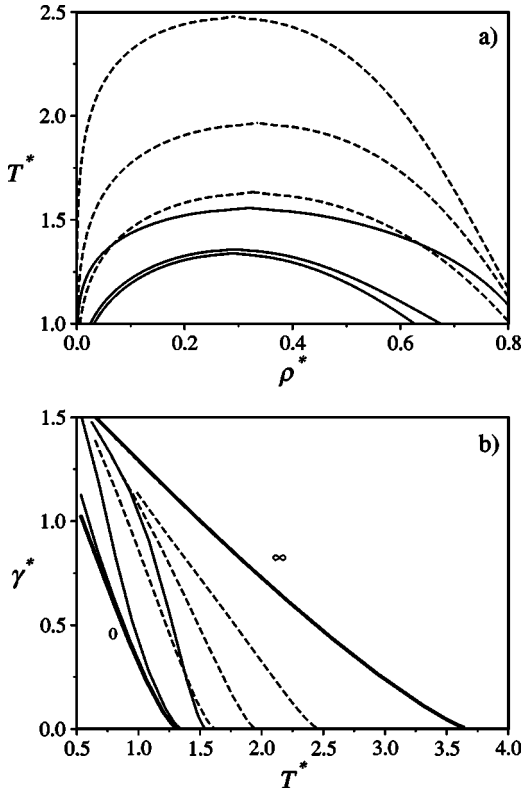

FIG. 10. (a) The vapor-liquid coexistence curve for an asymmetrical four-site associating (branched chain forming) square-well fluid (model 1:3), where $T^*=k_BT/\varepsilon$ and $\rho^*=\rho\sigma^3$ are the reduced temperature and number density, respectively. The predictions of the SAFT-VR approach [Eq. (3)] are represented by the curves: the continuous curves correspond to a small bonding volume of $K_{hb}^*=0.001$ (with $r_d^*=0.25$ and $r_c^*=0.5606$), and the dashed curves to a large bonding volume of $K_{hb}^*=0.1$ (with $r_d^*=0.25$ and $r_c^*=0.7631$). The site-site bonding interaction is $\varepsilon_{hb}^*=2$, 4, and 8 (curves from top to bottom). (b) The corresponding vapor-liquid surface tension $\gamma^*=\gamma\sigma^2/\varepsilon$ as a function of the reduced temperature. The curves represent the predictions of the SAFT-VR DFT [Eq. (26)]; see part a for details of the various systems. The limiting cases of the nonassociating ($\varepsilon_{hb}^*=0$) and fully associated dimer ($\varepsilon_{hb}^*=\infty$) systems are also shown as the thick continuous curves for reference.

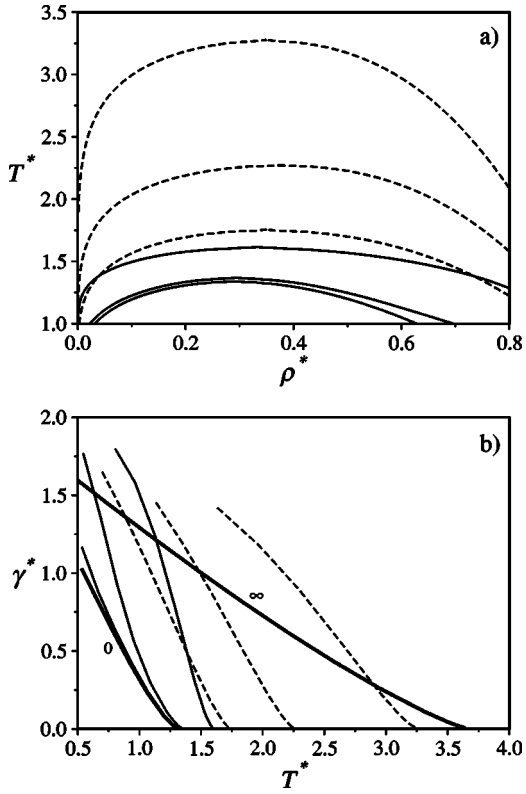

FIG. 11. (a) The vapor-liquid coexistence curve for a symmetrical four-site associating (network forming) square-well fluid (model 2:2), where $T^*=k_BT/\varepsilon$ and $\rho^*=\rho\sigma^3$ are the reduced temperature and number density, respectively. The predictions of the SAFT-VR approach [Eq. (3)] are represented by the curves: the continuous curves correspond to a small bonding volume of $K_{hb}^*=0.001$ (with $r_d^*=0.25$ and $r_c^*=0.5606$), and the dashed curves to a large bonding volume of $K_{hb}^*=0.1$ (with $r_d^*=0.25$ and $r_c^*=0.7631$). The site-site bonding interaction is $\varepsilon_{hb}^*=1$, 2, and 4 (curves from top to bottom). (b) The corresponding vapor-liquid surface tension $\gamma^*=\gamma\sigma^2/\varepsilon$ as a function of the reduced temperature. The curves represent the predictions of the SAFT-VR DFT [Eq. (26)]; see part a for details of the various systems. The limiting cases of the nonassociating ($\varepsilon_{hb}^*=0$) and fully associated dimer ($\varepsilon_{hb}^*=\infty$) systems are also shown as the thick continuous curves for reference.

ties of a wide variety of pure compounds is presented in a separate contribution.[92]

IV. CONCLUSION

We have developed an accurate Helmholtz free energy density functional theory (DFT) to describe the vapor-liquid interface of associating chain molecules, based on the statistical associating fluid theory for attractive potentials of variable range (SAFT-VR). The motivation of this work was to improve on the mean-field description of the attractive interactions employed in our earlier work.[26,34] One can incorporate the segment-segment correlations in the attractive perturbation term by using an average correlation function of the reference hard sphere system, and treat the other SAFT-VR contributions locally as a reference contribution. The resulting SAFT-VR DFT is shown to provide an excellent description of the vapor-liquid equilibria, interfacial profiles, and surface tension of square-well fluids of variable range. We have also compared the surface tension of a dimerizing square-well fluid obtained from the SAFT-VR DFT with recent simulation data and have found good agreement. As an alternative to the SAFT-VR DFT, one can treat the inhomogeneous fluid at the full SAFT-VR level and treat the attractive perturbation term at the mean-field level by including the short-range contribution to the attractive term in the reference term. Though the resulting SAFT-VR MF DFT approach does not provide as good a description of the interfacial properties as the full SAFT-VR DFT treatment, it represents a more general method. The mean-field treatment of the perturbation term in such an approach allows one to develop a general theory for the interfacial properties using an arbitrary engineering equation of state of the bulk fluid. In future work we plan to extend the SAFT-VR DFT to describe vapor-liquid and liquid-liquid interfaces in multicomponent mixtures.

The effect of different association schemes (dimerization, straight and branched chain formation, and network formation) on the interfacial properties has been examined in detail. The vapor-liquid surface tension of the associating fluid is found to be bounded between the nonassociating and

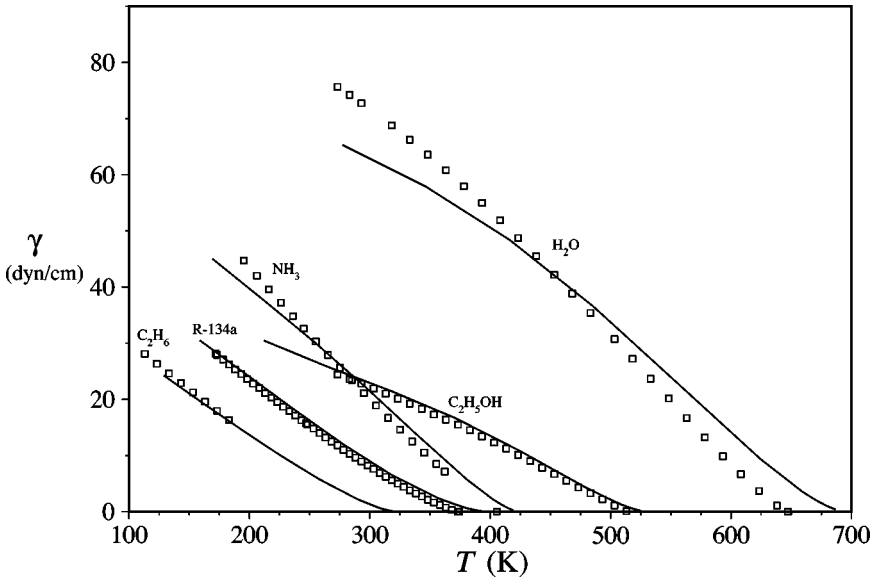

FIG. 12. The temperature dependence of the vapor-liquid surface tension (data points) γ for a selection of pure components: ethane (C_2H_6); the refrigerant 1,1,1,2-tetrafluoroethane (*R*134a); ammonia (NH_3); ethanol (C_2H_5OH); and water (H_2O). A preliminary comparison of the experimental data (Refs. 102 and 103) with the SAFT-VR DFT description [Eq. (26)] is made (see Refs. 70 and 92 for details).

fully associated limits, except for systems that associate into networks which exhibit a qualitatively different behavior. The shape of the temperature dependence is very sensitive to the balance between the strength and range of the association, and the precise association scheme. In the case of a system with a strong but very localized association interaction, the characteristic s-shaped surface tension curve seen in fluids such as water and alkanols can be reproduced. The various types of curves observed in real substances can be reproduced by the theory.

The adequacy of the SAFT-VR DFT in describing the vapor-liquid surface tension has been assessed briefly for a small number of real compounds. In the case of nonassociating molecules such as ethane, the intermolecular potential parameters obtained by optimizing the description of the bulk vapor-liquid phase equilibria (vapor pressure and saturated liquid density) also provide a good description of the surface tension. This indicates that a reasonably accurate surface tension can be obtained with a DFT approach of this kind without having to take into account the contributions due to capillary waves. This is in contrast with the findings of Winkelmann[15] who finds that the effect of capillary waves has to be included to adequately describe the surface tension of argon and nitrogen. The contribution of capillary waves to the interfacial tension is expected to be too small to be noticeable in three dimensions.[104] It is possible that the effect seen by Winkelmann is due in part to the specific intermolecular potential that were used. In the case of the associating compounds the magnitude of the surface tension will be dominated by the association and the effect of capillary waves will be even smaller in relative terms. A more complete comparison of our SAFT-VR DFT calculations with the vapor-liquid surface tension of a number of real compounds is given in Ref. 92.

ACKNOWLEDGMENTS

G.J.G. would like to thank the BP Exploration for funding a studentship, and F.J.B. would like to thank the Oil extraction Program of the Engineering and Physical Sciences Research Council (EPSRC) for the award of a research fellowship (Grant No. GR/N20317). We acknowledge further support from the EPSRC (Grant Nos. GR/N03358, GR/N35991, and GR/R09497), the Joint Research Equipment Initiative (JREI) for computer hardware (Grant No. GR/M94427), and the Royal Society-Wolfson Foundation for the award of a refurbishment grant. F.J.B., E.M.d.R., and E.d.M. are also grateful for financial support from Project No. BFM2001-1420-C02-02 of the Spanish DGICYT (Dirección General de Investigación Científica y Técnica), as well as for additional financial support from Universidad de Huelva and Junta de Andalucía.

[1] J. S. Rowlinson and F. L. Swinton, *Liquids and Liquid Mixtures*, 3rd. ed. (Butterworth Scientific, London, 1982).
[2] J. V. Senger, R. F. Kayser, C. J. Peter, and H. J. White, Jr., *Equations of State for Fluids and Fluid Mixtures* (Elsevier, Amsterdam, 2000), Vols. 1 and 2.
[3] W. G. Chapman, K. E. Gubbins, G. Jackson, and M. Radosz, Fluid Phase Equilib. **52**, 31 (1989).
[4] W. G. Chapman, K. E. Gubbins, G. Jackson, and M. Radosz, Ind. Eng. Chem. Res. **29**, 1709 (1990).
[5] M. S. Wertheim, J. Stat. Phys. **35**, 19 (1984).
[6] M. S. Wertheim, J. Stat. Phys. **35**, 35 (1984).
[7] M. S. Wertheim, J. Stat. Phys. **42**, 459 (1986).
[8] M. S. Wertheim, J. Stat. Phys. **42**, 477 (1986).
[9] E. A. Müller, and K. E. Gubbins, *A Review of SAFT and Related Approaches* in *Equations of State for Fluids and Fluid Mixtures*, edited by J. V. Sengers, R. F. Kayser, C. J. Peters, and H. J. White, Jr., (Elsevier, Amsterdam, 2000), Vol. 2.
[10] E. A. Müller and K. E. Gubbins, Ind. Eng. Chem. Res. **40**, 2193 (2001).
[11] J. S. Rowlinson and B. Widom, *Molecular Theory of Capillarity* (Clarendon, Oxford, 1982).
[12] J. D. van der Waals, Z. Phys. Chem. **13**, 657 (1894); J. Stat. Phys. **20**, 197 (1979).

[13] R. Evans, *Density Functionals in the Theory of Nonuniform Fluids* in *Fundamentals of Inhomogeneous Fluids*, edited by D. Henderson (Dekker, New York, 1992).
[14] H. T. Davis, *Statistical Mechanics of Phases and Interfaces, and Thin Films* (Wiley, VCH, Weinheim, 1996).
[15] J. Winkelmann, J. Phys.: Condens. Matter **13**, 4739 (2001).
[16] D. E. Sullivan, Phys. Rev. A **25**, 1669 (1982).
[17] S. Toxvaerd, J. Chem. Phys. **55**, 3116 (1971).
[18] S. Toxvaerd, Mol. Phys. **26**, 91 (1973).
[19] S. Toxvaerd, J. Chem. Phys. **64**, 2863 (1976).
[20] B. S. Carey, L. E. Scriven, and H. T. Davis, J. Chem. Phys. **69**, 5040 (1978).
[21] Z. X. Tang, L. E. Scriven, and H. T. Davis, J. Chem. Phys. **95**, 2659 (1991).
[22] S. Sokolowski and J. Fischer, J. Chem. Phys. **96**, 5441 (1992).
[23] T. Wadewitz and J. Winkelmann, J. Chem. Phys. **113**, 2447 (2000).
[24] Y. Tang and J. Wu, J. Chem. Phys. **119**, 7388 (2003); D. Fu and J. Wu, Mol. Phys. **102**, 1479 (2004).
[25] W. G. Chapman, Ph.D. Thesis Cornell University, Ithaca, 1988.
[26] F. J. Blas, E. Martín del Río, E. de Miguel, and G. Jackson, Mol. Phys. **99**, 1851 (2001).
[27] B. Yang, D. E. Sullivan, B. Tjipto-Margo, and C. G. Gray, J. Phys.: Condens. Matter **3**, 109 (1991).
[28] L. Mühlbacher, J. Chem. Phys. **108**, 10205 (1998).
[29] M. Borówko, L. Stepniak, S. Sokolowski, and R. Zagorski, Czech. J. Phys. **49**, 1067 (1999).
[30] V. Talanquer and D. W. Oxtoby, J. Chem. Phys. **112**, 851 (2000).
[31] O. Pizio, A. Patrykiejew, and S. Sokolowski, J. Chem. Phys. **113**, 10761 (2000).
[32] T. B. Peery and G. T. Evans, J. Chem. Phys. **114**, 2387 (2001).
[33] J. Alejandre, Y. Duda, and S. Sokolowski, J. Chem. Phys. **118**, 329 (2003).
[34] G. J. Gloor, F. J. Blas, E. Martín del Río, E. de Miguel, and G. Jackson, Fluid Phase Equilib. **194**, 521 (2002).
[35] G. Jackson, W. G. Chapman, and K. E. Gubbins, Mol. Phys. **65**, 1 (1988).
[36] W. G. Chapman, G. Jackson, and K. E. Gubbins, Mol. Phys. **65**, 1057 (1988).
[37] A. Galindo, P. J. Whitehead, G. Jackson, and A. N. Burgess, J. Phys. Chem. **100**, 6781 (1996).
[38] J. W. Cahn and J. E. Hilliard, J. Chem. Phys. **28**, 258 (1958).
[39] S. Abbas and S. Nordholm, J. Colloid Interface Sci. **166**, 481 (1994).
[40] P. M. W. Cornelisse, C. J. Peters, and J. de Swaan Arons, Fluid Phase Equilib. **117**, 312 (1996).
[41] H. Kahl and S. Enders, Fluid Phase Equilib. **172**, 27 (2000).
[42] D. Fu, J. F. Lu, T. Z. Bao, and Y. G. Li, Ind. Eng. Chem. Res. **39**, 320 (2000).
[43] C. McCabe and S. B. Kiselev, Ind. Eng. Chem. Res. **43**, 2839 (2004).
[44] J. C. Pàmies and L. F. Vega (unpublished); J. C. Pàmies, Ph.D. Thesis Universitat Rovirai Virgili, Taragona, 2003.
[45] C. Tapia-Medina, P. Orea, L. Mier-y-Teran, and J. Alejandre, J. Chem. Phys. **120**, 2337 (2004).
[46] J. K. Singh and D. A. Kofke, Mol. Simul. **30**, 343 (2004).
[47] A. Gil-Villegas, A. Galindo, P. J. Whitehead, S. J. Mills, G. Jackson, and A. N. Burgess, J. Chem. Phys. **106**, 4168 (1997).
[48] A. Galindo, L. A. Davies, A. Gil-Villegas, and G. Jackson, Mol. Phys. **93**, 241 (1998).
[49] C. McCabe, A. Gil-Villegas, and G. Jackson, J. Phys. Chem. B **102**, 4183 (1998).
[50] C. McCabe, A. Galindo, A. Gil-Villegas, and G. Jackson, J. Phys. Chem. B **102**, 8060 (1998).
[51] C. McCabe, A. Galindo, A. Gil-Villegas, and G. Jackson, Int. J. Thermophys. **9**, 1511 (1998).
[52] C. McCabe and G. Jackson, Phys. Chem. Chem. Phys. **1**, 2057 (1999).
[53] A. Galindo, A. Gil-Villegas, P. J. Whitehead, G. Jackson, and A. N. Burgess, J. Phys. Chem. B **102**, 7632 (1998).
[54] A. Galindo, A. Gil-Villegas, G. Jackson, and A. N. Burgess, J. Phys. Chem. B **103**, 10272 (1999).
[55] A. Galindo, L. J. Florusse, and C. J. Peters, Fluid Phase Equilib. **158**, 123 (1999).
[56] D. P. Visco and D. Kofke, Fluid Phase Equilib. **158**, 37 (1999).
[57] A. Galindo, S. J. Burton, G. Jackson, D. P. Visco, and D. Kofke, Mol. Phys. **100**, 2241 (2002).
[58] A. Galindo and F. J. Blas, J. Phys. Chem. B **106**, 4503 (2002).
[59] F. J. Blas and A. Galindo, Fluid Phase Equilib. **194**, 501 (2002).
[60] E. J. M. Filipe, E. J. S. G. de Azevedo, L. F. G. Martins, V. A. M. Soares, J. C. G. Calado, C. McCabe, and G. Jackson, J. Phys. Chem. B **104**, 1315 (2000).
[61] E. J. M. Filipe, L. F. G. Martins, J. C. G. Calado, C. McCabe, and G. Jackson, J. Phys. Chem. B **104**, 1322 (2000).
[62] C. McCabe, L. M. B. Dias, G. Jackson, and E. J. M. Filipe, Phys. Chem. Chem. Phys. **3**, 2852 (2001).
[63] R. P. Bonifacio, E. J. M. Filipe, C. McCabe, M. F. C. Gomes, and A. A. H. Padua, Mol. Phys. **100**, 2547 (2002).
[64] E. J. M. Filipe, L. M. B. Dias, J. C. G. Calado, C. McCabe, and G. Jackson, Phys. Chem. Chem. Phys. **4**, 1618 (2002).
[65] L. M. B. Dias, R. P. Bonifacio, E. J. M. Filipe, J. C. G. Calado, C. McCabe, and G. Jackson, Fluid Phase Equilib. **205**, 163 (2002).
[66] P. Paricaud, A. Galindo, and G. C. Maitland, Ind. Eng. Chem. Res. **42**, 3809 (2003).
[67] C. McCabe, A. Galindo, M. N. García-Lisbona, and G. Jackson, Ind. Eng. Chem. Res. **40**, 3835 (2001).
[68] P. Paricaud, A. Galindo, and G. Jackson, Fluid Phase Equilib. **194**, 87 (2002).
[69] P. Paricaud, A. Galindo, and G. Jackson, Ind. Eng. Chem. Res. **43**, 6871 (2004).
[70] G. J. Gloor, Ph.D. Thesis Imperial College London, 2003.
[71] G. J. Gloor, F. J. Blas, E. de Miguel, and G. Jackson, (unpublished).
[72] C. G. Gray and K. E. Gubbins, *Theory of Molecular Fluids* (Clarendon, Oxford, 1984).
[73] J. A. Barker and D. Henderson, J. Chem. Phys. **47**, 2856 (1967).
[74] J. A. Barker and D. Henderson, J. Chem. Phys. **47**, 4714 (1967).
[75] N. F. Carnahan and K. E. Starling, J. Chem. Phys. **51**, 635 (1969).
[76] J. P. Hansen and I. R. McDonald, *Theory of Simple Liquids*, 2nd ed. (Academic, London, 1986).
[77] J. A. Barker and D. Henderson, Rev. Mod. Phys. **48**, 587 (1976).
[78] W. G. Chapman, J. Chem. Phys. **93**, 4299 (1990).
[79] M. S. Wertheim, J. Chem. Phys. **87**, 7323 (1987).
[80] E. Kierlik and M. L. Rosinberg, J. Chem. Phys. **97**, 9222 (1992).
[81] E. Kierlik and M. L. Rosinberg, J. Chem. Phys. **99**, 3950 (1993).
[82] S. Phan, E. Kierlik, M. L. Rosinberg, A. Yethiraj, and R. Dickman, J. Chem. Phys. **102**, 2141 (1995).
[83] J. Gross and G. Sadowski, Fluid Phase Equilib. **168**, 183 (2000).
[84] J. Lekner and J. R. Henderson, Mol. Phys. **34**, 333 (1977).
[85] L. Vega, E. de Miguel, L. F. Rull, G. Jackson, and I. A. McLure, J. Chem. Phys. **96**, 2296 (1992).
[86] F. del Río, E. Ávalos, R. Espíndola, L. F. Rull, G. Jackson, and S. Lago, Mol. Phys. **100**, 2531 (2002).
[87] J. R. Henderson and F. van Swol, Mol. Phys. **56**, 1313 (1985).
[88] P. Orea, Y. Duda, and J. Alejandre, J. Chem. Phys. **118**, 5635 (2003).
[89] J. K. Singh, D. A. Kofke, and J. R. Errington, J. Chem. Phys. **119**, 3405 (2003).
[90] F. A. Escobedo and J. J. de Pablo, Mol. Phys. **87**, 347 (1996).
[91] E. A. Guggenheim, J. Chem. Phys. **13**, 253 (1945).
[92] G. J. Gloor, F. J. Blas, and G. Jackson (unpublished).
[93] W. R. Smith and I. Nezbeda, J. Chem. Phys. **81**, 3694 (1984).
[94] I. Nezbeda, J. Kolafa, and W. R. Smith, Fluid Phase Equilib. **130**, 133 (1997).
[95] I. Nezbeda, J. Pavlicek, J. Kolafa, A. Galindo, and G. Jackson, Fluid Phase Equilib. **158**, 193 (1999).
[96] C. Vega and L. G. MacDowell, Mol. Phys. **98**, 1295 (2000).
[97] F. J. Blas, A. Galindo, and C. Vega, Mol. Phys. **101**, 449 (2003).
[98] R. P. Sear, M. D. Amos, and G. Jackson, Mol. Phys. **80**, 777 (1993).
[99] W. Bol, Mol. Phys. **45**, 605 (1982).
[100] I. Nezbeda, J. Mol. Liq. **73**, 317 (1997).
[101] J. Slovak and I. Nezbeda, Mol. Phys. **101**, 789 (2003).
[102] B. D. Smith and R. Srivastava, *Physical Science Data*, **25**-*Thermodynamic Data for Pure Compounds* (Elsevier, New York, 1986).
[103] N. B. Vargaftik, *Tables on the Thermophysical Properties of Liquids and Gases in Normal and Dissociated States* (Hemisphere, London, 1975).
[104] M. P. Gelfand and M. E. Fisher, Physica A **166**, 1 (1990).